NPS-69SL76062

NAVAL POSTGRADUATE SCHOOL

Monterey, California

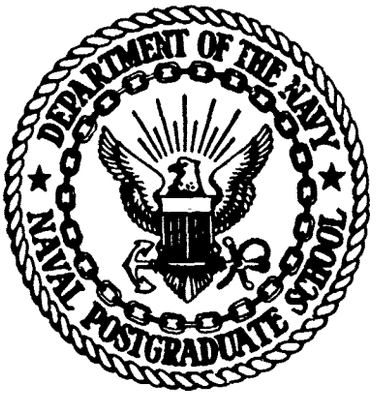

IN-LINE AND TRANSVERSE FORCES ON SMOOTH AND SAND-ROUGHENED CYLINDERS IN OSCILLATORY FLOW AT HIGH REYNOLDS NUMBERS

By

TURGUT SARPKAYA

4 June 1976

PREPARED FOR:
NATIONAL SCIENCE FOUNDATION, WASHINGTON, D. C. 20550.

NAVAL POSTGRADUATE SCHOOL
Monterey, California

Rear Admiral Isham Linder
Superintendent

J. R. Borsting
Provost

IN-LINE AND TRANSVERSE FORCES ON SMOOTH AND SAND-ROUGHENED CYLINDERS IN OSCILLATORY FLOW AT HIGH REYNOLDS NUMBERS

This report presents the results of an extensive experimental investigation of the in-line and transverse forces acting on smooth and sand-roughened circular cylinders placed in oscillatory flow at Reynolds numbers up to 1,500,000; Keulegan-Carpenter numbers up to 100; and relative sand-roughnesses from 1/800 to 1/50. The drag and inertia coefficients have been determined through the use of the Fourier analysis and the least-squares method. The transverse force (lift) has been analysed in terms of its maximum, semi peak-to-peak, and root-mean-square values. In addition, the frequency of vortex shedding and the Strouhal number have been determined.

The results have shown that (a) for smooth cylinders, all of the coefficients cited above are functions of the Reynolds and Keulegan-Carpenter numbers, particularly for Reynolds numbers larger than about 20,000; (b) for rough cylinders, the force coefficients also depend on the relative roughness k/D and differ significantly from those corresponding to the smooth cylinder; and that (c) the use of the 'frequency parameter' $D^2/\nu T$ and the roughness Reynolds number $U_m k/\nu$ allow a new interpretation of the present as well as the previously obtained data.

The work reported herein has been supported in part by The National Science Foundation through Grant No. AG-477.

This report was prepared by:

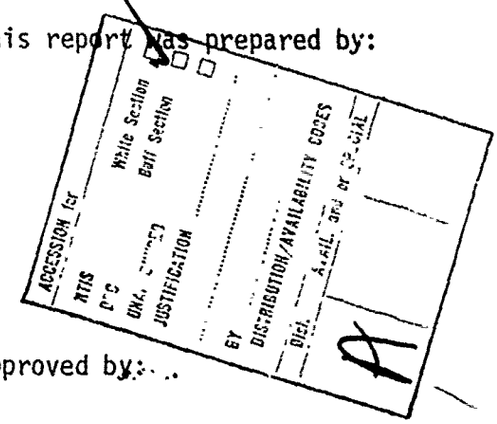

Turgut Sarpkaya
Distinguished Professor of
Mechanical Engineering

Approved by:

Allen E. Fuhs
Allen E. Fuhs, Chairman
Department of
Mechanical Engineering

Robert R. Fossum
Dean of Research

NPS-69SL76062

SECURITY CLASSIFICATION OF THIS PAGE *(When Data Entered)*

REPORT DOCUMENTATION PAGE

READ INSTRUCTIONS BEFORE COMPLETING FORM

1. REPORT NUMBER: (14) NPS-69SL76062
2. GOVT ACCESSION NO.
3. RECIPIENT'S CATALOG NUMBER: (9)

4. TITLE *(and Subtitle)*: (6) IN-LINE AND TRANSVERSE FORCES ON SMOOTH AND SAND-ROUGHENED CYLINDERS IN OSCILLATORY FLOW AT HIGH REYNOLDS NUMBERS.

5. TYPE OF REPORT & PERIOD COVERED: Interim Report. Feb [illegible] — June [illegible] 1976.

6. PERFORMING ORG. REPORT NUMBER

7. AUTHOR(s): (10) TURGUT SARPKAYA
DISTINGUISHED PROFESSOR OF MECHANICAL ENGINEERING

8. CONTRACT OR GRANT NUMBER(s): NATIONAL SCIENCE FOUNDATION Grant No. AG-477.

9. PERFORMING ORGANIZATION NAME AND ADDRESS
Naval Postgraduate School
Monterey, California 93940

10. PROGRAM ELEMENT, PROJECT, TASK AREA & WORK UNIT NUMBERS

11. CONTROLLING OFFICE NAME AND ADDRESS
National Science Foundation
Washington, D. C. 20550

(11)

12. REPORT DATE: 4 June [illegible] 1976
13. NUMBER OF PAGES

14. MONITORING AGENCY NAME & ADDRESS *(if different from Controlling Office)*: (12) 66p. (15) NSF-AG-477 OK

15. SECURITY CLASS. *(of this report)*: Unclassified

15a. DECLASSIFICATION/DOWNGRADING SCHEDULE

16. DISTRIBUTION STATEMENT *(of this Report)*

Approved for public release; distribution unlimited.

17. DISTRIBUTION STATEMENT *(of the abstract entered in Block 20, if different from Report)*

The source must be acknowledged in using or referring to the data presented in this report.

18. SUPPLEMENTARY NOTES

19. KEY WORDS *(Continue on reverse side if necessary and identify by block number)*

Oscillating Flow; Wave Forces; Drag and Inertia Coefficients; Roughened Cylinders; Harmonic Flow; Fluid Loading on Ocean Structures.

20. ABSTRACT *(Continue on reverse side if necessary and identify by block number)*

This report presents the results of an extensive experimental investigation of the in-line and transverse forces acting on smooth and sand-roughened circular cylinders placed in oscillatory flow at Reynolds numbers up to 7.5x10⁶, Keulegan-Carpenter numbers up to 100, and relative sand-roughnesses from 1/800 to 1/50. The drag and inertia coefficients have been determined through the use of the Fourier analysis and the least-squares method. The transverse force (lift) has been analysed in terms of its

1,500,000

DD FORM 1 JAN 73 1473 EDITION OF 1 NOV 65 IS OBSOLETE S/N 0102-014-6601 | 1

251 450

SECURITY CLASSIFICATION OF THIS PAGE *(When Data Entered)*

43

maximum, semi peak-to-peak, and root-mean-square values. In addition, the frequency of vortex shedding and the Strouhal number have been determined.

The results have shown that (a) for smooth cylinders, all of the coefficients cited above are functions of the Reynolds and Keulegan-Carpenter numbers, particularly for Reynolds numbers larger than about 20,000; (b) for rough cylinders, the force coefficients also depend on the relative roughness k/D and differ significantly from those corresponding to the smooth cylinder; and that (c) the use of the 'frequency parameter' $D^2/\nu T$ and the roughness Reynolds-number $U_m k/\nu$ allow a new interpretation of the present as well as the previously obtained data.

TABLE OF CONTENTS

LIST OF FIGURES

NOMENCLATURE

A	Amplitude of oscillations at the test section
A_o	Amplitude of oscillations at the free surface
C_d	Drag coefficient
C_L	Maximum lift coefficient
C_m	Inertia coefficient
D	Diameter of the test cylinder
F	Force
F_d	Drag force
F_i	Inertia force
f	Frequency of oscillations, $1/T$
f_v	Frequency of vortex shedding, (first harmonic)
g	Gravitational acceleration
H	Elevation, (see Fig. 1)
K	Keulegan-Carpenter number, $U_m T/D$
k	Roughness height
L	Length of the test cylinder
p	Pressure
Re	Reynolds number, $U_m D/\nu$
T	Period of oscillations in the tunnel
t	Time
U	Instantaneous velocity
U_m	Maximum velocity in a cycle
$U_m k/\nu$	Roughness Reynolds number
β	Frequency parameter, $D^2/\nu T$
γ	Specific weight of water
θ	$2\pi t/T$
ν	Kinematic viscosity of water at a given temperature
ρ	Density of water

ACKNOWLEDGMENTS

The work described in this report represents part of a research program supported by the Engineering Division of the National Science Foundation through Grant No. AG-477. This support is gratefully acknowledged.

The writer is indebted to the many people whose co-operation made this investigation possible. Messrs. N. J. Collins, S. R. Evans, and D. Henning, all graduate Students at the Naval Postgraduate School, assisted with the experiments and data evaluation. Mr. Jack McKay, an artist and ingenious model maker, built all the critical parts of the instrumentation. The computer time was donated by the Naval Postgraduate School.

This report is dedicated to Hans von Nikolausberg for his lifelong friendship.

INTRODUCTION

The design of structures for the marine environment requires the prediction of the forces generated by waves and currents. Much of the present knowledge has been obtained by means of model tests at Reynolds numbers generally two to three orders of magnitude smaller than prototype Reynolds numbers. These model tests have relied heavily on the so-called Morison formula for expressing the force as the sum of a drag and inertia force. The values of the drag and inertia coefficients to be used in the Morison equation became the subject of many experimental studies in the last twenty years. The correlation of these coefficients with the relative amplitude of the waves (or the Keulegan-Carpenter number) has been generally inconclusive. The complexity of the problem stems partly from the difficulty of accurately defining the kinematics of the flow field, partly from the difficulty of accounting properly for the effects of time-dependent separation and vortex shedding, and partly from the difficulty in extrapolating the laboratory findings to various conditions of the marine environment where three-dimensional effects and reduced spanwise coherence play important roles. It thus became clear that much is to be gained by considering plane oscillatory flow about cylinders at high Reynolds numbers in order to isolate the influence of individual factors such as relative amplitude, Reynolds number, and the relative roughness on vortex shedding and resistance. It is with this realization that the present investigation was undertaken and the preliminary results obtained with smooth cylinders in a small U-shaped water tunnel operating at relatively low Reynolds numbers (2,500 to 25,000) have been previously reported [1].

The present paper deals with in-line and transverse forces acting on smooth and sand-roughened circular cylinders in harmonic flow at critical and transcritical Reynolds numbers.

APPARATUS AND PROCEDURE

Of the two possible methods of generating relative harmonic fluid motion about bluff bodies, namely, oscillating the fluid or the body, the former has been chosen. The relative merits and shortcomings of the two methods have been amply discussed [2] and will not be repeated here. Suffice it to note that large amplitude structural and free-surface oscillations commonly enccuntered in oscillating the body in a fluid otherwise at rest do not lead to reliable data. The advantages of the apparatus used herein for the purpose under consideration have already been demonstrated [1, 2] and will become further evident from the data to be presented.

The oscillating flow system consisted of a large U-shaped vertical water tunnel as shown in Fig. 1. The cross-section of the two vertical legs is 3 ft by 6 ft and that of the test section is 3 ft by 3 ft. The two corners of the tunnel were carefully streamlined to prevent flow separation. This design proved to be more than adequate for no separation was encountered, and also the desired frequency and amplitude of oscillation were achieved. The auxiliary components of the tunnel consisted of plumbing for hot and cold water, butterfly-valve system, and the air-supply system.

The butterfly-valve system (mounted on top of one of the legs of the tunnel) consisted of four plates, each 18 inches wide and 36 inches long. All four valves were simultaneously driven by a simple rack and pinion

system actuated by an air-driven piston and a three-way pneumatic valve. Initially, the bucterfly valves were closed and air was introduced to that side of the tunnel, with an electrically-controlled ball valve, to create the desired differential water level between the two legs of the tunnel. Then the valves were opened with the help of the rack and pinion system and the three-way control valve. This action set the fluid in the tunnel in oscillatory motion with a natural period of T = 5.500 seconds. The elevation, acceleration, and all force traces were absolutely free from secondary oscillations so that no filters whatsoever were used between the outputs of the transducers and the recording equipment (see Fig. 2).

Throughout the investigation, the monitoring of the characteristics of the oscillations in the tunnel was of prime importance in view of the fact that most of the difficulties in the past in the determination of the drag, lift, and inertia coefficients resulted from the difficulty of generating a purely harmonic motion free from vibrations or from applying theoretically derived rather than measured values for velocities and accelerations.

Three transducers were used to generate three independent d.c. signals, each proportional to the instantaneous value of elevation, velocity, and acceleration. The first one consisted of a platinum wire stretched vertically in one leg of the tunnel. The response of the wire was perfectly linear within the range of oscillations encountered. The second method consisted of the measurement of the instantaneous acceleration by means of a differential-pressure transducer connected to two pressure taps placed horizontally 2 ft apart and 4 ft to one side of the test section. The instantaneous acceleration was then calculated from $\Delta p = \rho s.dU/dt$ where

Δp is the differential pressure, s the distance between the pressure taps, and dU/dt is the instantaneous acceleration of the fluid. The third method again consisted of the measurement of the differential pressure between two pressure taps placed symmetrically on the two vertical legs of the tunnel at an elevation H ft below the mean water level. The linear differential-pressure transducer yielded the instantaneous elevation and hence the amplitude of oscillation since, according to Bernoulli's equation

$$A = 2A_o = [\Delta p/\gamma]_{max}/[1 - (2\pi/T)^2 H/g] \qquad (1)$$

in which g and T are constant and H is kept constant.

All three methods gave nearly identical results and yielded the amplitude A, the maximum velocity $U_m = 2\pi A/T$, or the maximum acceleration $a_m = (2\pi/T)^2 A$ to an accuracy of about 2 percent relative to each other. In addition to the methods cited above, the velocity at the test section was directly measured with a calibrated magnetic velocimeter. These comparisons, as well as the perfectly sinusoidal and noise-free character of all pressure and force traces, speak for the suitability of the unique test facility used in this study. The additional details of the apparatus and procedure are given in [2].

The in-line and transverse forces were measured with two identical, cantilever type, force transducers, one at each end of the cylinder. The gages had a capacity of 250 lbs and the deflection of the cantilever end was less than 0.008 inches. A special housing was built for each gage so that it can be mounted on the tunnel window and rotated to measure either the in-line or the transverse force alone. The test cylinders were placed

in the test section by retracting the gages from their housing and then pushing them into the bearings mounted on each end of the cylinders. This allowed a gap of 1/32 inch between the cylinder and the tunnel wall. The natural frequency of the cylinder and force-transducer combination in water was about 20 times larger than the frequency of oscillation of the water column and about 10 times larger than the largest frequency of vortex shedding.

Seven circular cylinders with diameters ranging in size from 2 inches to 6.5 inches were used. The cylinders were turned on a lathe from aluminum pipes or plexiglass rods and polished to a mirror-shine surface. Same cylinders were also used as rough cylinders. For this purpose, sand was sieved to obtain the desired relative roughness and applied uniformly on the cylinder surface with an air-drying epoxy paint. After a series of tests with water at various temperatures, the cylinders were polished again and covered with sand of different size. This procedure was continued until the desired ranges of all the governing parameters were covered.

Previously [2], sand paper, sand, and polystyrene beads were used as roughness elements for a given cylinder in order to achieve the desired relative roughness in a given Reynolds number range. A detailed study of the effective roughness of each type of roughness element and the discussions with the manufacturer have shown that the effective roughness of the sand paper is larger than the height of the mean sand particles applied on it. Furthermore, the gluing of the sand paper on the cylinder invariably resulted in a 'joint' along the cylinder which might have generated larger disturbances and promoted earlier transition. The polystyrene beads, on the other hand, present an effective-roughness

height which is often smaller than their actual size [3]. In spite of these differences, however, the terminal values of the drag coefficients in the transcritical region remained practically the same for a given actual effective relative roughness whether the data were obtained with sand alone or with a combination of other roughness elements. Evidently, it will be most interesting and desirable to carry out similar experiments with cylinders roughened in the ocean environment. The results presented herein show that the testing of roughened cylinders with steady uniform flow is not sufficient for the purposes under consideration, namely the determination of the fluid loading on offshore structures.

FORCE COEFFICIENTS AND GOVERNING PARAMETERS

Data reduction for the forces in-line with the direction of oscillation is based on Morison equation [4] and three different analysis of the force records, namely, Fourier analysis, least squares, and a modified least squares method.

The in-line force which consists of the drag force F_d and the inertia force F_i is assumed to be given by [4]

$$F=F_d+F_i=0.5C_dLD\rho|U|U+0.25C_mLD^2\pi\rho.dU/dt \qquad (2)$$

in which C_d and C_m represent respectively the drag and inertia coefficients and U the instantaneous velocity of the ambient flow. For an oscillating flow represented by $U = -U_m \cos\theta$, with $\theta = 2\pi t/T$, the Fourier averages of C_d and C_m are given by Keulegan and Carpenter as [5]

$$C_d = -0.75 \int_0^{2\pi} (F_m \cos\theta / \rho U_m^2 LD)\, d\theta \qquad (3)$$

and

$$C_m = (2U_m T/\pi^3 D) \int_0^{2\pi} (F_m \sin\theta / \rho U_m^2 LD)\, d\theta \qquad (4)$$

in which F_m represents the measured force.

The method of least squares consists of the minimization of the error between the measured and calculated forces. This proceduer yields [6]

$$C_{dls} = -(8/3\pi) \int_0^{2\pi} (F_m |\cos\theta| \cos\theta / \rho DLU_m^2)\, d\theta \qquad (5)$$

and $C_{mls} = C_m$. Evidently, the Fourier analysis and the method of least squares yield identical C_m values and that C_d values differ only slightly. The details of the modified least-squares method may be found in [6] and will not be repeated here.

The transverse force has been expressed in terms of various coefficients. Some of these are: (a) the maximum lift coefficient defined by C_L = (maximum amplitude of the transverse force in a cycle)/$(0.5\rho LDU_m^2)$; (b) the semi peak-to-peak value of the transverse force normalized as above; and (c) the normalized root-mean-square value of the transverse force. In addition, the frequency of the oscillations of the transverse force and the Strouhal number have been evaluated.

It is recognized that the coefficients cited above are not constant throughout the cycle and are either time-invariant averages or peak values at a particular moment in the cycle. A simple dimensional analysis of the flow under consideration shows that the time-dependent coefficients may be written as

$$F/(0.5LD\rho U_m^2) = f(U_m T/D,\ U_m D/\nu,\ k/D,\ t/T) \qquad (6)$$

in which F represents the in-line or the transverse force. Equation (6), combined with Eq. (2), assuming for now that the latter is indeed valid, yields

$$C_d = f_1(K, Re, k/D, t/T) \qquad (7)$$

$$C_m = f_2(K, Re, k/D, t/T) \qquad (8)$$

in which $K = U_m T/D$ and $Re = U_m D/\nu$, and k/D represents the relative roughness.*

There is no simple way to deal with Eqs. (7) and (8) even for the most manageable time-dependent flows. Another and perhaps the only other alternative is to eliminate time as an independent variable and consider suitable time-invariant averages as given by Eqs. (3), (4), and (5).

---

*The one-parameter characterization of the effect of roughness needs some justification. It is of course recognized that not only the relative size of the roughness elements but also their shape and distribution may be quite important. It is in fact partly for the difficulty of uniquely specifying the 'roughness' and partly for the differences in other test conditions that there are considerable differences between the steady-flow data reported by various workers [7-10], particularly in the drag crisis region. For example, the effective surface roughness may be larger or smaller than the nominal relative roughness based on the geometric size of the roughness element depending on the shape and arrangement of the roughness elements [3]. It is partly for this reason that it has been thought advisable to investigate afresh the effect of roughness on cylinders in harmonic flow using only sand of uniform size and packing rather than three different types of roughness elements, (see Fig. 3 for sample photographs of the sand-roughened surfaces).

Thus, one has

$$[C_d , C_m , C_L , \ldots] = f_i(K , Re , k/D) \qquad (9)$$

It appears, for the purposes of Eq. (9), that the Reynolds number is not the most suitable parameter involving viscosity. The primary reasons for this are that the effect of viscosity is relatively small and that U_m appears in both K and Re. Thus, replacing Re by $Re/K = D^2/\nu T$ in Eq. (9), one has

$$C_i[\text{a coefficient}] = f_i(K , \beta , k/D) \qquad (10)$$

in which $\beta = D^2/\nu T$ and shall be called the 'frequency parameter'.

From the standpoint of dimensional analysis, either the Reynolds number or β could be used as an independent variable. Evidently, β is constant for a series of experiments conducted with a cylinder of diameter D in water of uniform and constant temperature since T is kept constant in a U-shaped oscillating flow tunnel. Then the variation of a force coefficient with K may be plotted for constant values of β. Subsequently, one can easily recover the Reynolds number from $Re = \beta K$ and connect the points, on each β = constant curve, representing a given Reynolds number.

From the standpoint of laminar boundary layer theory, β represents the ratio of the rate of diffusion of vorticity through a distance δ (the boundary-layer thickness) to the rate of diffusion through a distance D. This ratio is also equal to $(D/\delta)^2$ and, when it is large, gradients of velocity in the direction of flow are small compared with the gradients normal to the boundary, a situation to which the boundary-layer theory is applicable [11]. It should be noted in passing that the added mass and drag coefficients for a cylinder or sphere undergoing harmonic oscillations

without separation in a fluid otherwise at rest are determined uniquely in terms of β [11].

Let us now re-examine a set of data previously obtained by others [5] partly to illustrate the use and significance of β as one of the governing parameters and partly to take up the question of the effect of Reynolds number on the force coefficients.

The data given by Keulegan and Carpenter [5] may be represented by 12 different values of β. The drag and inertia coefficients are plotted in Figs. 4 and 5 and connected with straightline segments. Evidently, the identification of the individual data points in terms of the cylinder diameter, as was done by Keulegan and Carpenter [5] and also by Sarpkaya [1], irrespective of the β values gives the impression of a scatter in the data and invites one to draw a mean drag curve through all data points. Such a temptation is further increased by the fact that the data for each β span over only a small range of K values. Evidently, the drawing of such a mean curve eliminates the dependence of C_d and/or C_m on β and hence on Re.

Also shown in Figs. 4 and 5 are points representing four selected Reynolds numbers. The corresponding K values for each Re and β were calculated from $K = Re/\beta$. The points corresponding to the selected Reynolds numbers are reproduced in Figs. 6 and 7. These figures show, within the range of Re and K values encountered in Keulegan-Carpenter data, that (a) C_d depends on both K and Re and decreases with increasing Re for a given K; and that (b) C_m depends on both K and Re for K larger than approximately 15 and <u>decreases</u> with increasing Re. A similar analysis of Sarpkaya's data [1] also shows that C_d and C_m depend on both K and Re and that C_m <u>increases</u> with increasing Re. Notwithstanding this difference in the variation of C_m between the two

sets of data, Figs. 6 and 7 put to rest the long standing controversy regarding the dependence or lack of dependence of C_d and C_m on Re and show the importance of β as one of the governing parameters in interpreting the data, in interpolating the K values for a given Re, and in providing guide lines for further experiments as far as the ranges of K and β are concerned.

RESULTS AND DISCUSSIONS

Drag and Inertia Coefficients for Smooth Cylinders -

Only the representative data will be presented herein for sake of brevity. The tabulated as well as plotted data for all force coefficients for smooth circular cylinders are given in [2].*

Figures 8 and 9 show C_d versus K and C_m versus K for five representative values of β. Evidently, there is very little scatter in the data even though the figures represent the results of four independent runs. Mean lines drawn through the data shown in Figs. 8 and 9 are presented in Figs. 10 and 11 together with the constant Reynolds number lines obtained through the use of $K = Re/\beta$. Evidently, there is a remarkable correlation between the force coefficients, Reynolds number, and the Keulegan-Carpenter number. The smoothness of the constant Re lines is another indication of the consistency of the data from one cylinder to another.

---

*Additional data obtained since the writing of Ref. [2] are included herein in the figures showing C_d and C_m as a function of the Reynolds number for constant values of K and/or k/D.

Figures 10 and 11 show that C_d and C_m do not vary appreciably with Re for Re smaller than about 20,000 and help to explain the conclusions previously reached by Keulegan and Carpenter [5] and Sarpkaya [1].

The entire data, obtained since the inception of the investigation about five years ago, are shown as a function of Re for constant values of K in Figs. 12 and 13. These figures clearly show that C_d decreases with increasing Re to a value of about 0.5 (depending on K) and then gradually rises to a constant transcritical value within the range of Reynolds numbers encountered. The inertia coefficient C_m increases with increasing Re, reaches a maximum, and then gradually approaches a value of about 1.75. It will be recalled that the Keulegan-Carpenter data indicated an opposite trend. It is believed that the Keulegan-Carpenter data for C_m are not quite reliable for $K > 15$. This is also evident from the observation that the data corresponding to $\beta = 141$ appear to be out of place (see Fig. 5) relative to those corresponding to $\beta = 97$ and $\beta = 217$. Suffice it to say that the results presented in Figs. 12 and 13 shed new light on the variations of the drag and inertia coefficients and partly explain the reasons for the large scatter encountered in the plots of C_d versus Re and C_m versus Re as compiled by Wiegel [12].

Drag and Inertia Coefficients for Sand-Roughened Cylinders -

In view of the fact that each coefficient depends on at least three independent parameters (Re, K, and k/D), it is not possible to show on two-dimensional plots the variation of either C_d or C_m for all values of Re, K, and k/D. However, this difficulty is alleviated by the fact that the variation of a given force coefficient for a given Re and k/D is not

very strong from one K to another. Thus it has been decided to choose five representative K values, namely K = 20, 30, 40, 60, and 100, to present the variation of C_d and C_m with Re for five representative k/D values.

Figures 14 through 18 show C_d and C_m for five values of K as a function of the Reynolds number. Each curve on each plot corresponds to a particular relative roughness. Also shown on each figure is the corresponding drag or inertia coefficient for the smooth cylinder at the corresponding K value.

The k/D = constant curves on each C_d plot are quite similar to those found for steady flow about rough cylinders [7-10]. For a given relative roughness, the drag coefficient does not significantly differ from its smooth cylinder value at very low Reynolds numbers. As the Reynolds number increases, C_d for the rough cylinder decreases rapidly, goes through the region of 'drag crisis' at a Reynolds number considerably lower than that for the smooth cylinder and then rises sharply to a nearly constant transcritical value. The larger the relative roughness the larger is the magnitude of the minimum C_d and the smaller is the Reynolds number at which that minimum occurs. However, there appears to be a minimum Reynolds number below which the results for rough cylinders do not significantly differ from those corresponding to smooth cylinders. In other words, the Reynolds number must be sufficiently high for the roughness to play a role on the drag and flow characteristics of the cylinder.

The figures for the drag coefficient also exhibit a few other interesting features. First, even a relative roughness as small as 1/800 can give rise to transcritical drag coefficients which are considerably higher than those for the smooth cylinder. Secondly, the asymptotic values of the drag coefficient for roughened cylinders within the range of Reynolds numbers

encountered, can reach values which are considerably higher than those obtained with steady flows over cylinders of similar roughness ratio. In other words, it is not safe to assume that the transcritical drag coefficient in harmonic flows will be identical to those found in steady flows and will not exceed a value of about unity. On the basis of the present results it may be said that such a conjecture is not accurate even for K values as large as 100 (corresponding to a wave height-to-diameter ratio of about 30). In steady flow about a cylinder, roughness precipitates the occurrence of 'drag crisis' and gives rise to a minimum drag coefficient which is larger than that obtained with a smooth cylinder [7-10]. This is partly because of the transition to turbulence of the free shear layers at relatively lower Reynolds numbers (due to disturbances brought about by the roughness elements) and partly because of the retardation of the boundary-layer flow by roughness (higher skin friction) and, hence, earlier separation. In harmonic flow about a cylinder, roughness appears to play an even more complex role because of the time-dependence of the boundary layer and the position of the separation points. In particular, the magnitude of the transverse force (to be discussed subsequently) strongly suggests that the combined effect of uniformly-distributed roughness and time dependence (even in the drag dominated region of K values) is to increase the strength of vortices and the spanwise coherence relative to that in steady flow at the same Re about the same cylinder.

The Reynolds number at which the drag crisis occurs gives rise to an 'inertia crisis'. In other words, for a given relative roughness, C_m rises rapidly to a maximum at a Reynolds number which corresponds to that at which C_d drops to a minimum. At relatively higher Reynolds numbers, C_m decreases

somewhat and then attains nearly constant values which are lower than those corresponding to the smooth cylinders. It is also apparent from the inertia coefficient curves that the smaller the relative roughness the larger is the maximum inertia coefficient. For relatively smaller roughnesses such as k/D = 1/800, the terminal value of C_m is nearly equal to that of a smooth cylinder. The behavior of C_m is not entirely unexpected. It has long been noted [5] that whenever there is a rise in the drag coefficient, there also is a decrease in the inertia coefficient.

Before closing the discussion of the drag and inertia coefficients, it is necessary to point out the remarkably consistent behavior of the data points, particularly for C_d. Perhaps it would not have been too surprising had the data been obtained for one relative roughness through the use of only one cylinder. In the present investigation, the use of several cylinders and several temperatures for a given cylinder always provided data for nearly identical k/D, Re, and K values. For instance, the C_d and C_m values obtained at a given K, Re, and relative roughness k/D, using a 5 inch cylinder at a low temperature corresponds to the C_d and C_m values using a 4-in. cylinder at a high temperature. Remembering the fact that not only the actual size of the cylinders but also the size of the sand grains differed in order to obtain the same k/D, and the fact that the experiments were carried out at different temperatures and times, one fully realizes that the correlation of the data and the relatively small scatter are indeed quite remarkable. This is due not only to the repeatability of the tests but also due to the vibration-free operation of the entire tunnel system.

The correlation length along the cylinders was not directly measured.

However, one series of experiments was conducted with a 2.18-diameters (12 inches) long, centrally located, section of a 5.5-inch cylinder which 'floated' on the ends of the force transducers with small gaps (0.002 in.) between the section and the rest of the rigidly supported 12-inch long sections. The floating and dummy sections were carefully polished and tested as a smooth cylinder. Then both sections were coated with sand for a relative roughness of k/D = 1/100. The comparison of the lift, drag, and inertia coefficients obtained with the short section with those obtained with the longer section spanning the entire test section has shown that the two sets of coefficients are nearly identical for both smooth and roughened cylinders. The differences were in the order of experimental errors and, if anything, the drag coefficients obtained with the short section were about 3% larger than those obtained with the 3-foot section. Evidently, the force-cancelling effects of phase shifts which may have been brought about by three-dimensional effects were either insignificant or non-existent. Thus, it is concluded that both the three-dimensionality effects and the boundary-layer effects played very little or no role in the present investigation.

A comparison of the results shown in Figs. 14 through 18 with the previously reported [2, 13] preliminary results for roughened cylinders for K = 50 alone indicates that the type of roughness may affect the variation of the drag coefficient with Reynolds number, particularly in the drag-crisis region. Previously, sand paper, sand, and polystyrene beads were used [2] as roughness elements for a given cylinder in order to achieve the desired relative roughness in a given Reynolds number range. In spite of the differences in the 'effective roughness' of the three types of roughness elements, however, the terminal values of the drag coefficients

in the transcritical region remained practically the same for a given actual effective relative roughness whether the data were obtained with sand alone or with a combination of other roughness elements. Evidently, it will be most interesting and desirable to carry out similar experiments with cylinders roughened in the ocean environment.

In-Line Force Coefficients and the Roughness Reynolds Number -

The data given in Figs. 18a and 18b are replotted in Fig. 19 as a function of the roughness Reynolds number defined by $U_m k/\nu$ for all values of k/D. Similar plots may be prepared for other values of K through the use of Figs. 14 through 17.

It is rather remarkable that C_d and C_m become practically independent of k/D for $U_m k/\nu$ larger than about 300. In other words, for sufficiently large values of the roughness Reynolds number, the drag and inertia coefficients for a roughened cylinder in a given harmonic flow are determined by the height of the excrescences rather than by the diameter of the cylinder. The importance and the consequences of this result are self evident for supercritical Reynolds number simulation for flow over circular cylinders. A detailed discussion of this and other pertinent concepts for steady flow over roughened cylinders is presented by Szechenyi [10] and will not be repeated here.

Transverse Force and Vortex Shedding for Smooth and Rough Cylinders -

The data for the maximum lift coefficient for smooth cylinders are summarized in Figs. 20 and 21. The original data in plotted and tabulated form are presented in [2]. Evidently, the lift coefficient depends on Re for Re larger than about 20,000 and rapidly decreases to about 0.2 for

larger values of Re and K. It is also evident that the lift force is a major portion of the total force acting on the cylinder and cannot be neglected in the design of structures.

The frequency of the alternating transverse force is shown in Fig. 22 in terms of $f_r = f_v/f$ as a function of K and Re. It is apparent that f_r is not constant and increases with increasing K and Re. Furthermore, a quick calculation through the use of Fig. 22 shows that the Strouhal number given by $St = f_v D/U_m = f_r/K$ is not constant at 0.2, as in steady flow, and depends on both Re and K.

Several additional facts are of special importance in connection with the variation of the lift coefficient and the frequency ratio. Firstly, the lift curve begins at K = 5. There is an occasional vortex shedding for K values between 4 and 5. The minimum value of K at which lift or asymmetry in the vortices develops is, by the very nature of vortices, extremely sensitive to the experimental conditions. Evidently, what is of special importance is not the highest value of K at which the symmetry of the vortices can be maintained with extreme care but the lowest value of K below which asymmetry cannot be initiated in spite of the magnitude of the external disturbances. A careful analysis of all the lift traces has shown that there is a 90% chance that the asymmetry will occur at K = 5. At K = 4, there is only a 5% chance that the asymmetry will appear for very short periods of time. Secondly, each $f_r = N$ line does not represent an absolute line of demarcation between the frequencies N-1 and N+1. Occasionaly, a frequency of N+1 will occur on the N-1 side of the N line, and vice versa. Thirdly, the frequency of vortex shedding is not a pure multiple of the frequency of flow oscillation. Evidently, f_r, as an integer, is a measure of the number

of vortices actually shed during a cycle. However, all of the vortices are not fully developed or completely shed. Thus, the fractional part of f_r indicates an incomplete vortex shedding. This phenomenon is particularly common for f_r values in the neighborhood of 3 and also for large values of K and Re where the oscillations of the transverse force become quite irregular. The significance of the foregoing relative to the in-line force will be taken up separately.

The maximum lift coefficient for the roughened cylinders are presented in Fig. 23 as a function of K for various values of β and one particular value of k/D. Additional details may be found in [14]. Evidently, C_L does not vary appreciably with either β or Re. The data presented in [14] for other values of k/D show that C_L does not vary with k/D also within the range of the parameters encountered. If there is some variation with these parameters (Re and β), it is certainly masked by the scatter of the data resulting from the random nature of the lift force. In fact, it is not too uncommon to obtain a variation of 20-25% for a given value of K. This fact is of importance in discussing the effect of the Reynolds number on the lift coefficient. Also shown in Fig. 23 is the lift coefficient for smooth cylinders for β in the range of 1000 to 2000. It is rather surprising that the smooth cylinder data at relatively low values of β form more or less the upper limit of the rough cylinder data. In other words, the lift coefficient for rough cylinders does not depend on Re and becomes almost identical to that for smooth cylinders at very low Reynolds numbers. The consequences of this observation for model testing purposes are rather obvious. The behavior of the lift coefficient for rough cylinders is in conformity with the fact that the transcritical drag coefficient for rough cylinders (steady or harmonic flow) nearly returns to its subcritical value.

As noted earlier, the alternating nature of the transverse force is as important as its magnitude. It is for this reason that the frequency of the lift force has been determined for rough cylinders also. A close examination of the frequency ratios shows that f_r/K remains essentially constant at a value of about 0.22 [14]. To be sure, there are variations from one cylinder to another and from a given combination of Re and K to another. Nevertheless, the Strouhal number is fairly constant for all roughnesses, relative amplitudes, and Reynolds numbers larger than about 20,000. This fact is of special importance in determining the in-line and transverse vibrational response of the elements of a structure to wave-induced forces. One must, however, keep in mind the fact that the spanwise coherence along a vertical cylinder in the ocean environment may be reduced by the variation of the velocity vector with time and depth and that the lift coefficients presented herein represent the maximum possible values of the transverse force.

ON THE APPLICABILITY OF MORISON'S EQUATION AND THE PRESENT DATA

Since its inception, questions have been raised regarding the applicability of Morison's equation to time-dependent flows in general and to wavy flows in particular. It has been known that the equation predicts quite accurately the in-line force for both very small values of K (K smaller than about 10) and for large values of K (K larger than about 20). For intermediate values of K, differences have been observed between the measured and calculated values. These differences have been attributed either to the imprecise measurement of the kinematics of the flow or to the shortcomings of the equation. It is now realized that not only these two factors (namely the heuristic nature of the equation and the difficulty of measuring the local

velocities and accelerations) but also the three-dimensional nature of the wavy flows and decreased spanwise coherence must be partly responsible for the differences between the measured and calculated forces. In fact, it would have been extremely difficult to draw meaningful conclusions regarding the applicability of Morison's equation through the use of the field data. It is only through the use of carefully conducted two-dimensional harmonic flow experiments that one can ascertain the degree of applicability of Morison's equation.

Figure 24 shows the calculated and measured forces normalized by $0.5DL\rho U_m^2$ together with the normalized velocity and the difference between the measured and calculated forces for a relatively large value of k/D. It is evident that there is often a remarkable correspondence between the measured and calculated forces particularly for K values larger than about 20. This is also true for K smaller than about 10. In the disturbance-sensitive region of vortex formation and onset of asymmetry, the growth and shedding of single or alternating vortices have profound effects not only on the measured in-line force but also on the force coefficients calculated. The fractional shedding of vortices and the vortex-induced oscillations in the in-line force give rise to an asymmetry in the magnitude of the in-line force. In other words, the in-line force can no longer be represented by an odd harmonic function. Thus, it is clear that part of the reason for the larger differences between the measured and calculated forces even in perfectly two-dimensional harmonic flows is due to the use of the force coefficients which are derived by assuming the in-line force to be given by an odd harmonic function. In the range of K values from about 10 to 20, particularly for low values of Re, this assumption is not quite correct as evidenced by the present experiments, (see also Ref. [2]).

In considering the relevance of the coefficients presented herein and of the equation devised by Morison to wave induced loads on offshore structures, it is of course important to take into account the differences between uniform two-dimensional harmonic motion and the wave motion where the velocity vector both rotates with time at a point and decays in magnitude with depth. The spanwise variations of the flow in general lead to reduced spanwise coherence. It is safe to assume that both the three-dimensionality of the flow and the reduction of the correlation length along the cylinder, in an ocean environment, tend to increase the base pressure and thus give rise to transcritical drag coefficients which are smaller than those obtained with purely two-dimensional flows. The drag coefficients presented herein obviously represent their maximum possible values since they have resulted from a uniform, two-dimensional flow where the instantaneous wake of the cylinder has the highest possible degree of spanwise coherence. The similarity between the reduced drag coefficient due to reduced spanwise coherence in wavy flows and the drag coefficient in steady flows (both for roughened cylinders) is rather fortuitous and does not imply the equality of the two drag coefficients in the drag-dominated region of the K values. It is rather unfortunate that even the experiments with wavy flows cannot be expected to isolate the effect of reduced spanwise coherence since such experiments surely bring in other factors whose influence is combined in a complex way with that of the reduced correlation. Thus, the value of the results presented herein lies in the fact that the designer now knows the maximum possible value of the coefficients under consideration, if not the values which might be more appropriate to the conditions under which the structure must survive and function.

CONCLUSIONS

The results presented herein warrant the following conclusions: (a) For smooth cylinders, the drag, lift, and the inertia coefficients depend on both the Reynolds and Keulegan and Carpenter numbers; (b) For roughened cylinders, the drag and inertia coefficients depend on Re, K, and k/D; (c) The drag coefficient undergoes a 'drag crisis' and rises to a nearly constant value (depending on k/D) within the range of Reynolds and Keulegan-Carpenter numbers tested; (d) The asymptotic values of the drag coefficient for $K < 100$ are larger than the transcritical drag coefficients for roughened cylinders in steady flow; (e) The results show that neither the acceleration modulus $R_1 = 2\pi/K$ nor the ratio of the maximum inertial force to maximum drag force $R_2 = (\pi^2/K)(C_m/C_d)$ is small enough (for the K, Re, and k/D values tested) for the harmonic flow to behave like a pseudo-steady flow over a roughened cylinder, (e.g. for K = 100, Re = 1,000,000, and k/D = 1/100, one has $C_d = 1.55$, $C_m = 1.6$, and $R_1 = 0.063$, $R_2 = 0.10$); (f) The importance of the role played by roughness in harmonic flow is further evidenced by the fact that in the same range of K and Re values, the transcritical C_d values for steady and harmonic flows become nearly identical even though the force ratio R_2 may be larger than that for the rough cylinder case, (e.g. for K = 100, Re = 1,000,000, one has $C_d = 0.65$, $C_m = 1.75$, and $R_1 = 0.063$, and $R_2 = 0.27$); (g) The physical mechanism responsible for the surprisingly large effect of roughness on resistance in flows with relatively small accelerations and decelerations needs careful study; (g) The inertia coefficient also undergoes an 'inertia crisis' at Re values corresponding to the 'drag crisis' at which C_m reaches a maximum value and then asymptotically decreases; (h) The drag and inertia coefficients become independent of k/D for roughness Reynolds numbers larger than about 300; (i) The transverse

force is a significant fraction of the total resistance at all Reynolds numbers for both smooth and rough cylinders and must be taken into consideration in the design of structures; (j) The Strouhal number for smooth cylinders depends on both K and Re. For rough cylinders, it remains nearly constant for all Reynolds numbers at about 0.22; (k) The results presented herein and the conclusions arrived at are applicable only to cylinders in harmonic flow with zero mean velocity within the range of the Re, K, and k/D values encountered in the tests. The force coefficients for wavy flows (with or without a mean velocity superimposed on them) may differ somewhat from those presented herein partly due to the reduced coherence along the length of the cylinder, partly due to the three-dimensionality of the flow, and partly due to the nonlinear interaction between the current and the waves. It is thus hoped that the data and the discussions presented herein will draw serious attention to the effect of roughness, three dimensionality, and spanwise coherence in wavy flows and will accentuate the need for additional laboratory and full scale experiments.

REFERENCES

1. Sarpkaya, T., "Forces on Cylinders and Spheres in a Sinusoidally Oscillating Fluid", Journal of Applied Mechanics, ASME, Vol. 42, No. 1, March 1975, pp. 32-37.

2. Sarpkaya, T., "Vortex Shedding and Resistance in Harmonic Flow About Smooth and Rough Cylinders at High Reynolds Numbers", Naval Postgraduate School Technical Report No. NPS-59SL76021, February 1976, Monterey, California 93940.

3. Schlichting, H., Bounday-Layer Theory, McGraw-Hill Book Co., N. Y., 1968, (6-th Ed.), p. 587.

4. Morison, J. R., et al., "The Force Exerted by Surface Waves on Piles", Petroleum Trans., Vol. 189, 1950, pp. 149-157.

5. Keulegan, G. H. and Carpenter, L. H., "Forces on Cylinders and Plates in an Oscillating Fluid", Journal of Research of the National Bureau of Standards, Research Paper No. 2857, Vol. 60, No. 5, May 1958.

6. Sarpkaya, T., "Forces on Cylinders Near a Plane Boundary in a Sinusoidally Oscillating Fluid", Fluid Mechanics in the Petroleum Industry, ASME, December 1975, pp. 43-47.

7. Fage, A. and Warsap, J. H., "The Effects of Turbulence and Surface Roughness on the Drag of a Circular Cylinder", ARC R and M 1283, 1929.

8. Achenbach, E., "Influence of Surface Roughness on the Cross-Flow Around a Circular Cylinder", Journal of Fluid Mechanics, Vol. 46, Pt. 2, 1971, pp. 321-335.

9. Guven, O. et al., "Surface Roughness Effects on the Mean Flow Past Circular Cylinders", Iowa Inst. of Hydraulic Research Report No. 175, May 1975, Iowa City.

10. Szechenyi, E., "Supercritical Reynolds Number Simulation for Two-Dimensional Flow Over Circular Cylinders", Journal of Fluid Mechanics, Vol. 70, Pt. 3, 1975, pp. 529-542.

11. Rosenhead, L. (Ed.), Laminar Boundary Layers, Oxford at the Clarendon Press, 1963, p. 393.

12. Wiegel, R. L., Oceanographical Engineering, Prentice Hall, Inc., Englewood Cliffs, N. J., 1964, pp. 257-260.

13. Sarpkaya, T., "In-Line and Transverse Forces on Cylinders in Oscillatory Flow at High Reynolds Numbers", Offshore Technology Conference, Paper No. 2533, May 1976.

14. Collins, N. J., "Transverse Forces on Smooth and Rough Cylinders in Harmonic Flow at High Reynolds Numbers", Thesis presented to the Naval Postgraduate School, Monterey, Calif., June 1976.

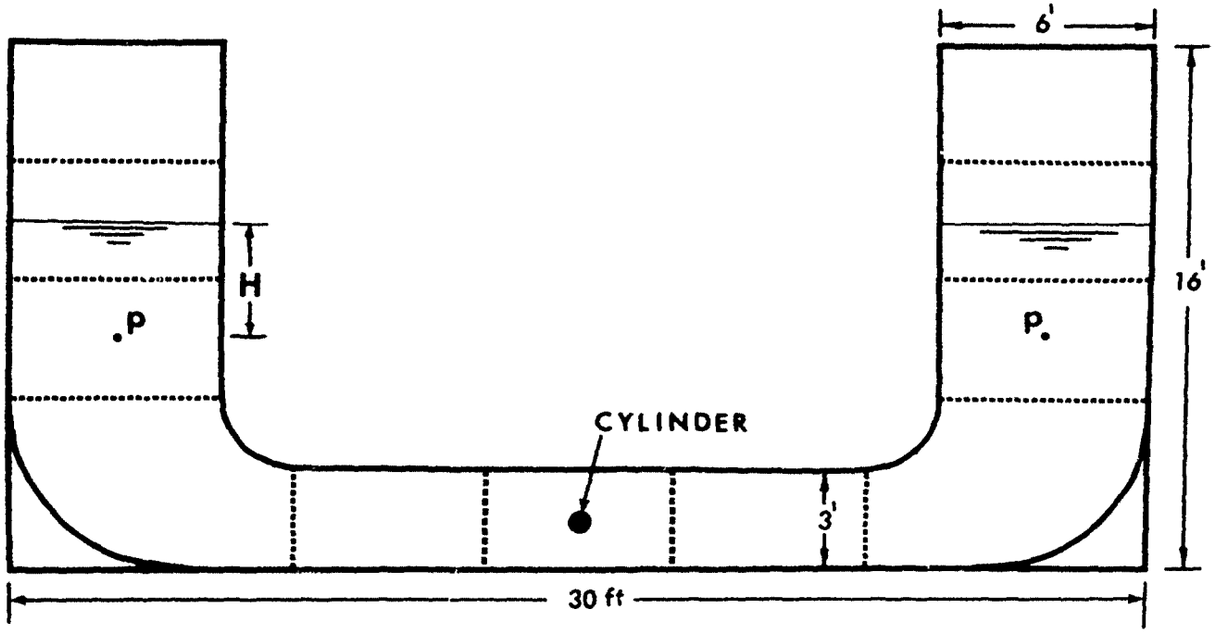

Fig. 1a Schematic drawing of the U-shaped vertical water tunnel.

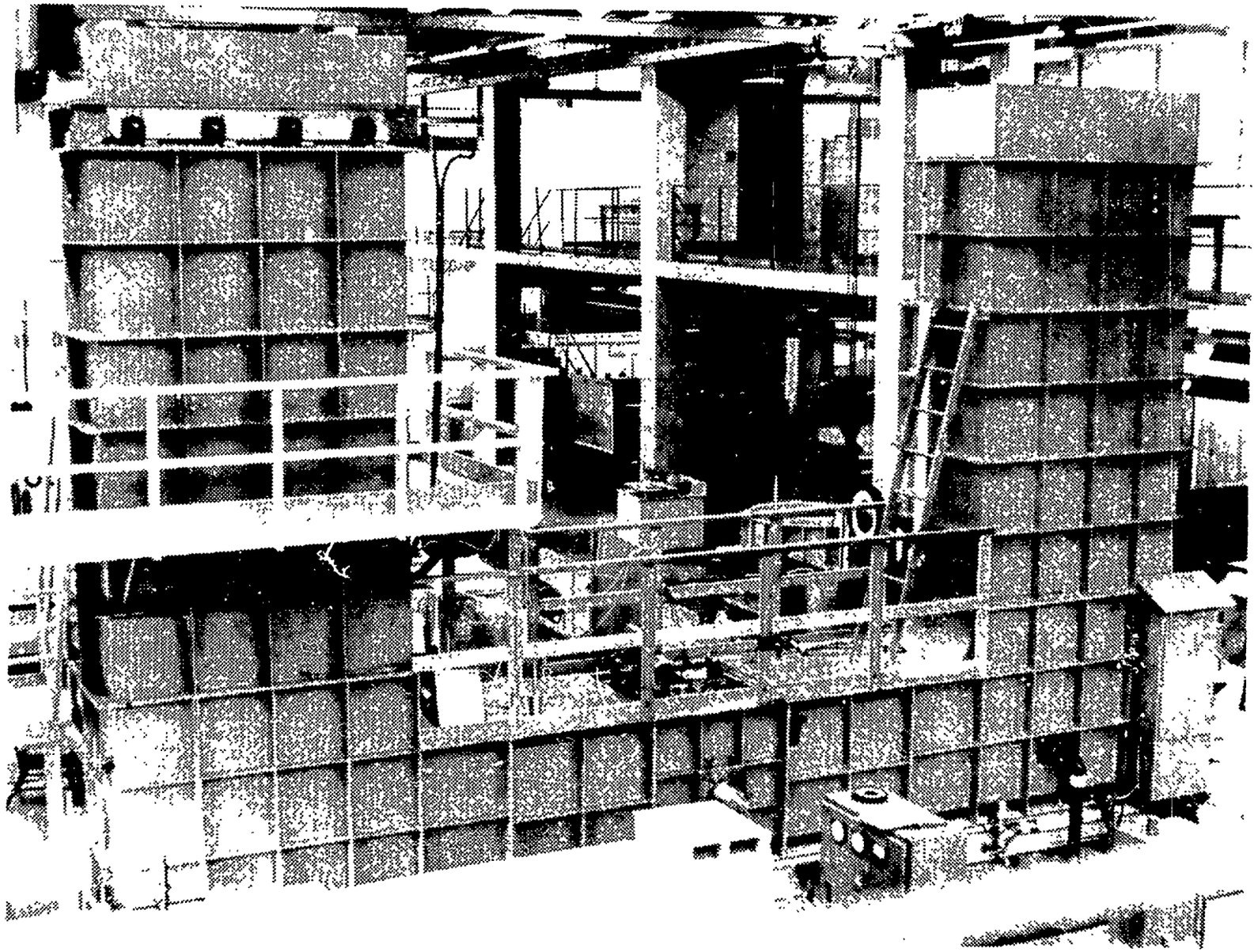

Fig. 1b general view of the U-shaped vertical water tunnel

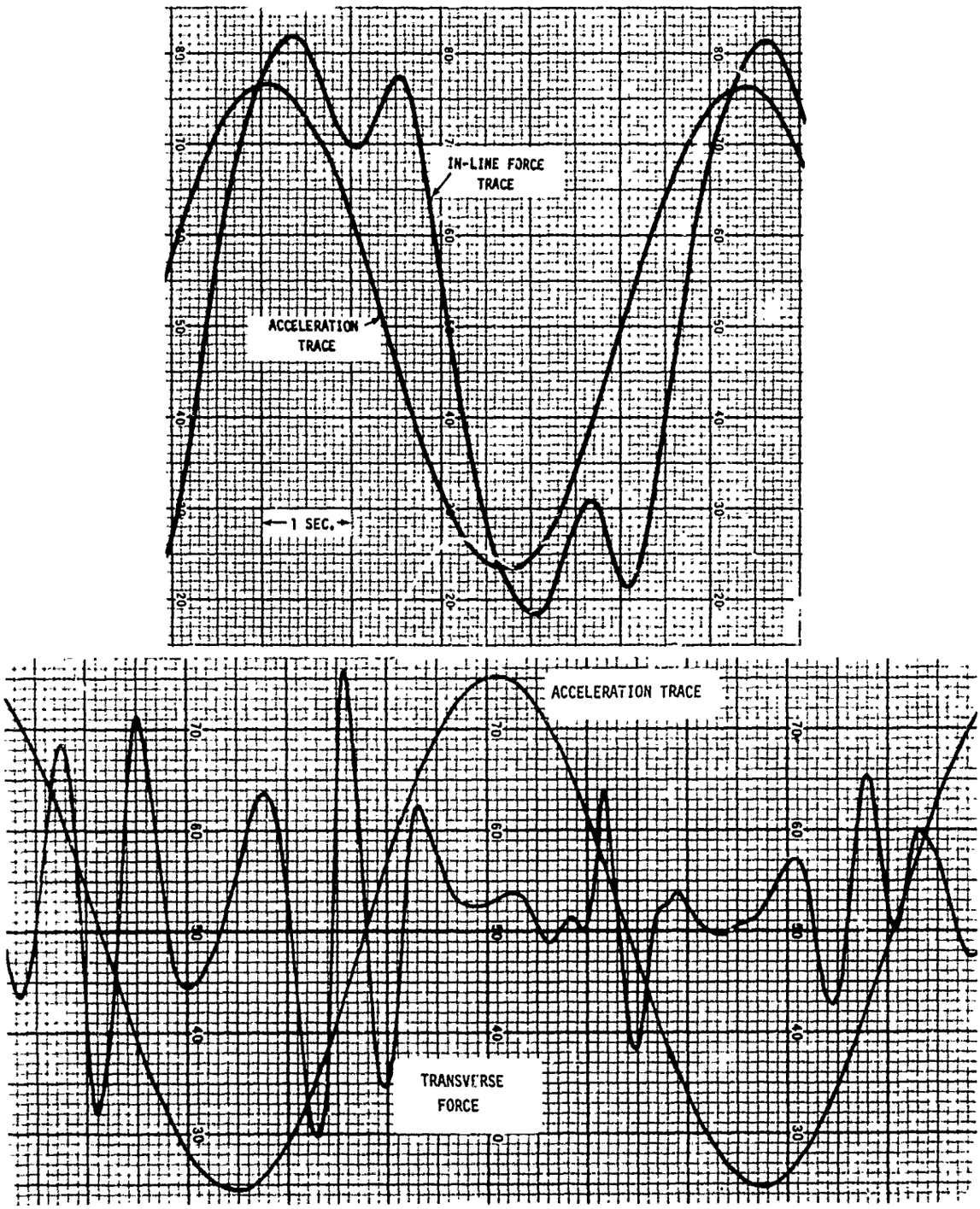

Fig. 2 Force and Acceleration Traces

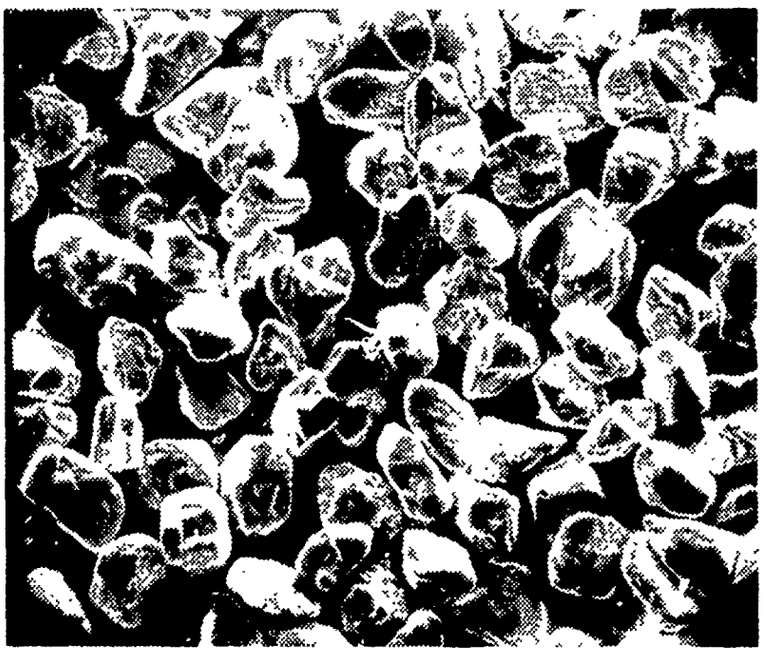

k = 0.018"

20-X

k = 0.018"

50-X

Fig. 3 Scanning Electron Microscope Photographs of Sand-Roughened Surface

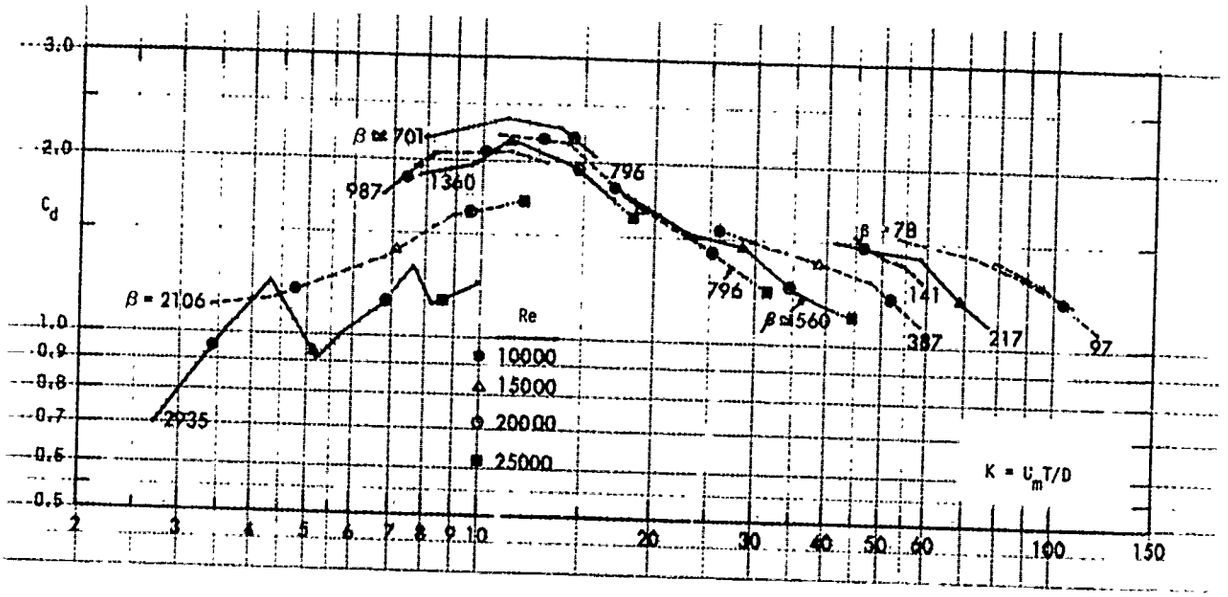

Fig. 4 C_d versus K for various values of β for the data provided by Keulegan and Carpenter [5]

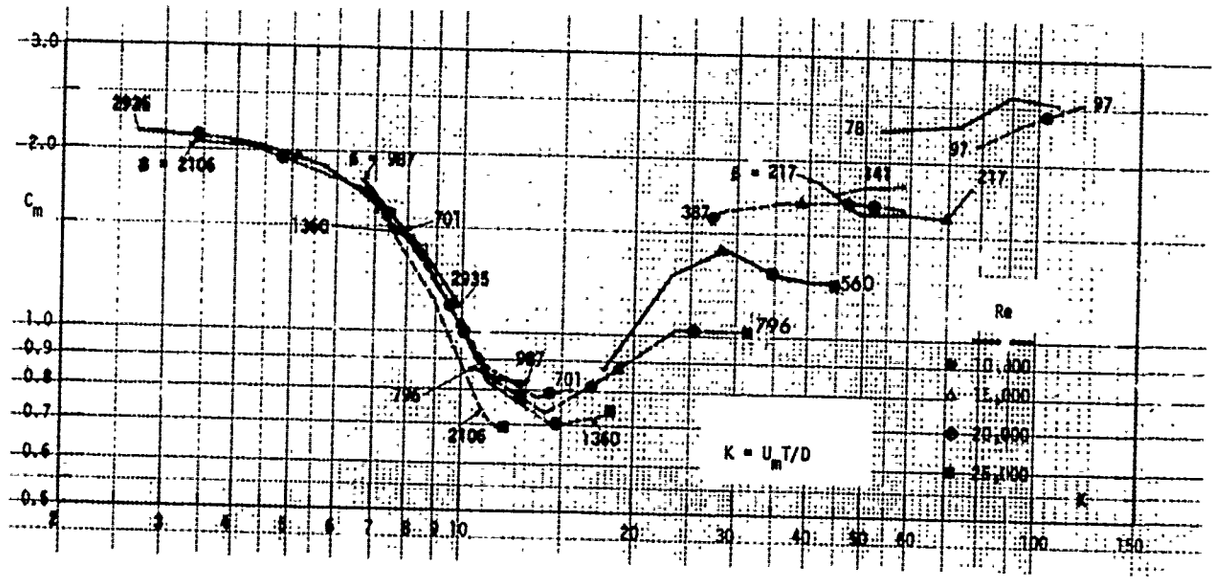

Fig. 5 C_m versus K for various values of β for the data provided by Keulegan and Carpenter [5]

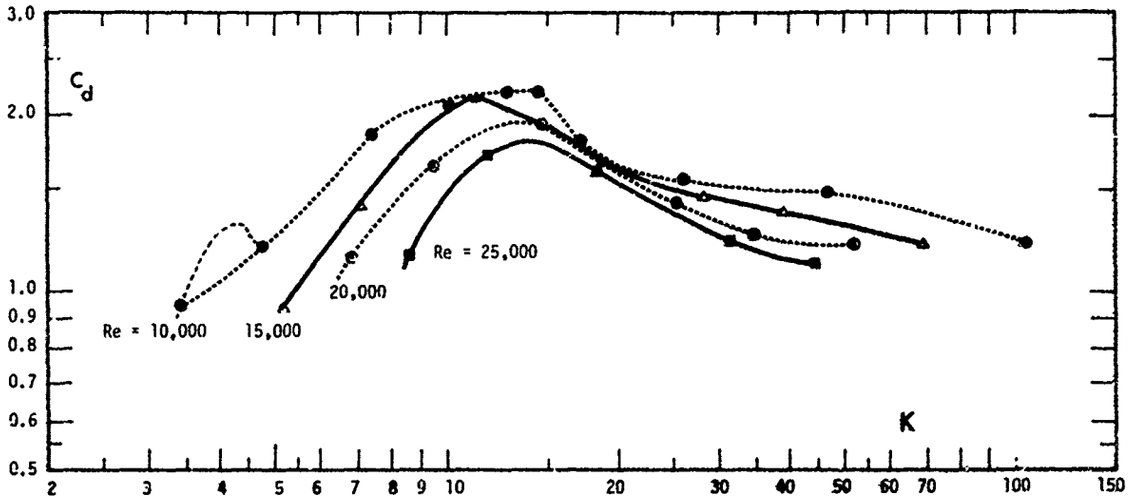

Fig. 6 C_d versus K for Constant Values of Re for the Data Provided by Keulegan and Carpenter [5]

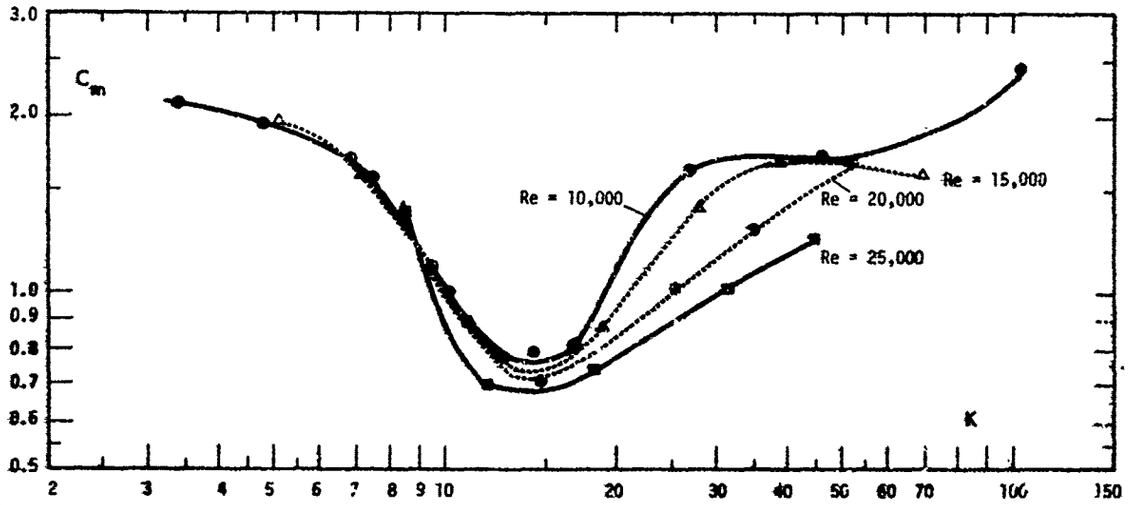

Fig. 7 C_m versus K for Constant Values of Re for the Data Provided by Keulegan and Carpenter [5]

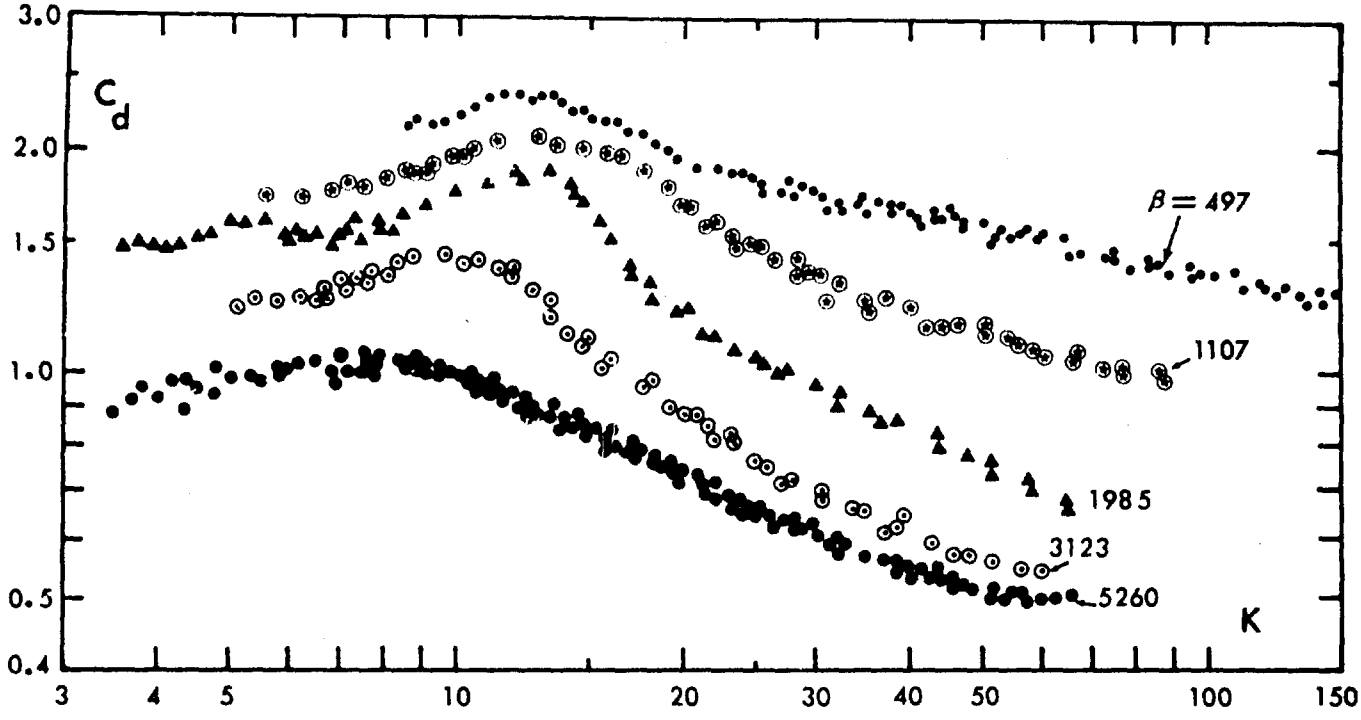

Fig. 8 C_d versus K for various values of β, (present data).

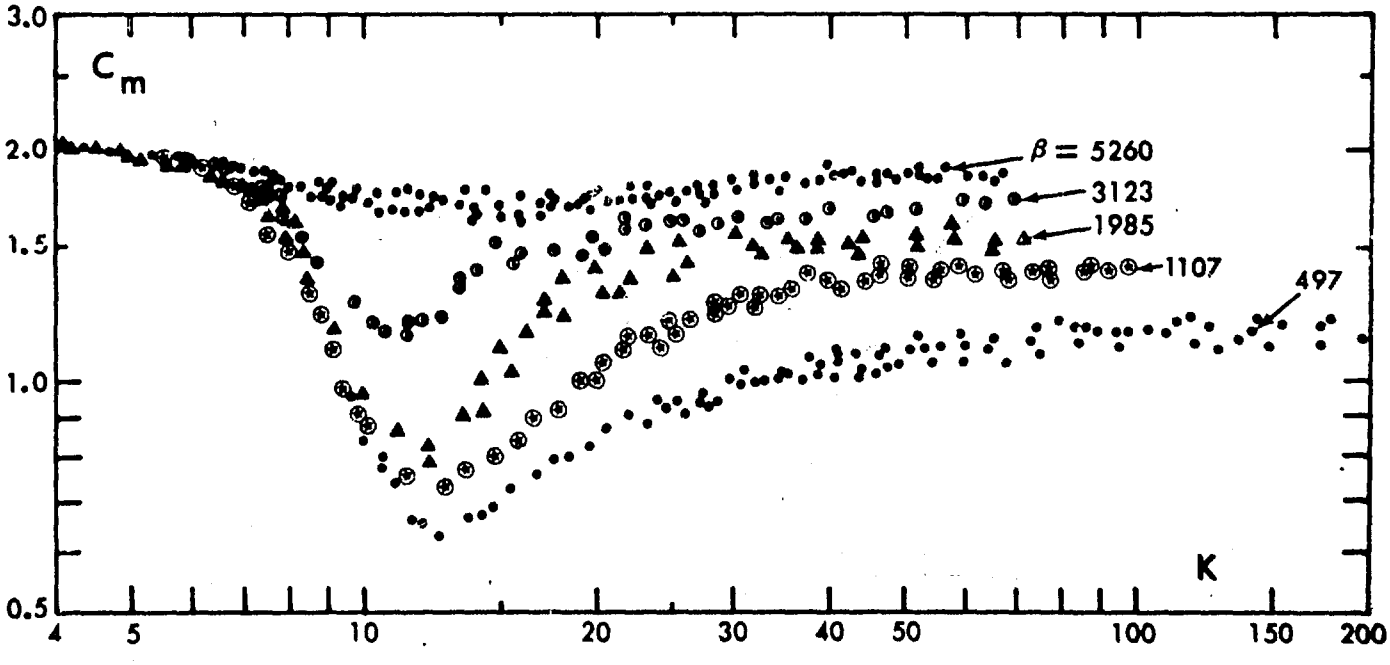

Fig. 9 C_m versus K for various values of β, (present data).

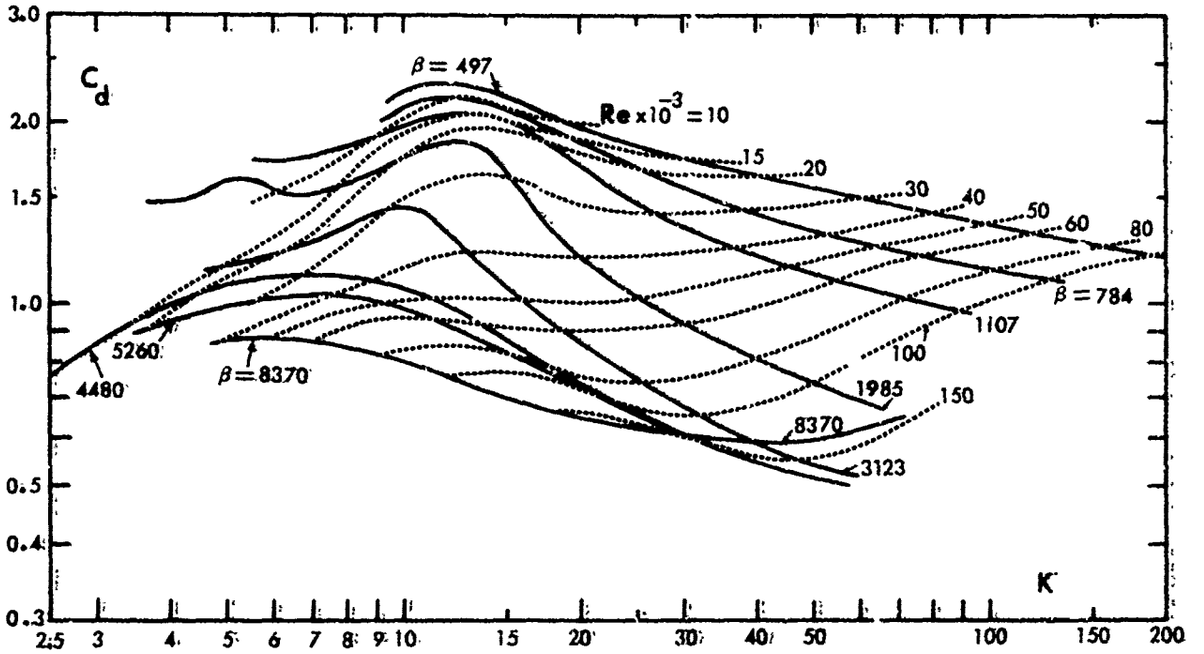

Fig. 10 C_d versus K for constant values of Re and β
(present data)

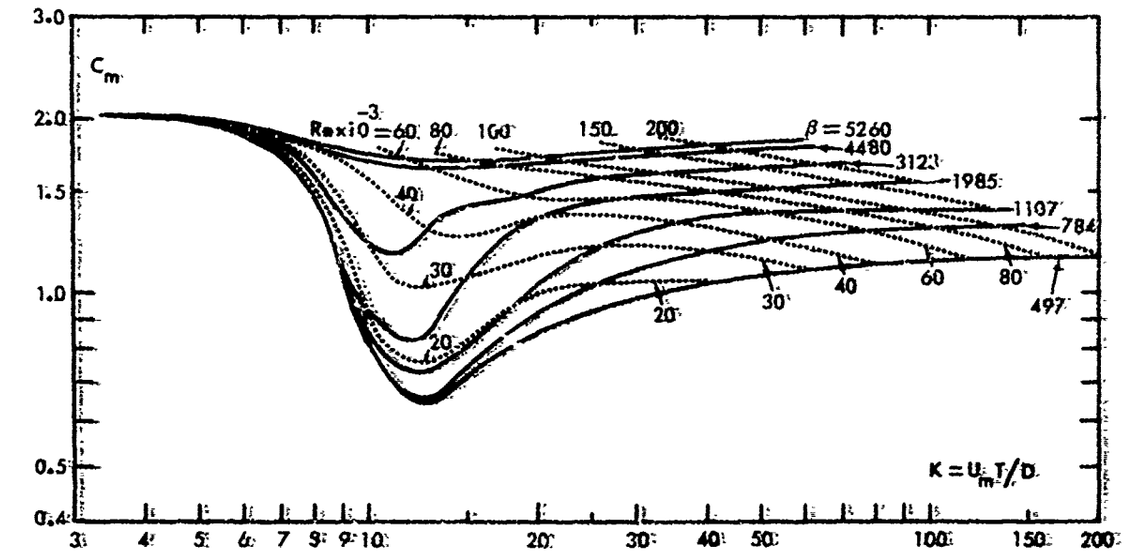

Fig. 11 C_m versus K for constant values of Re and β
(present data)

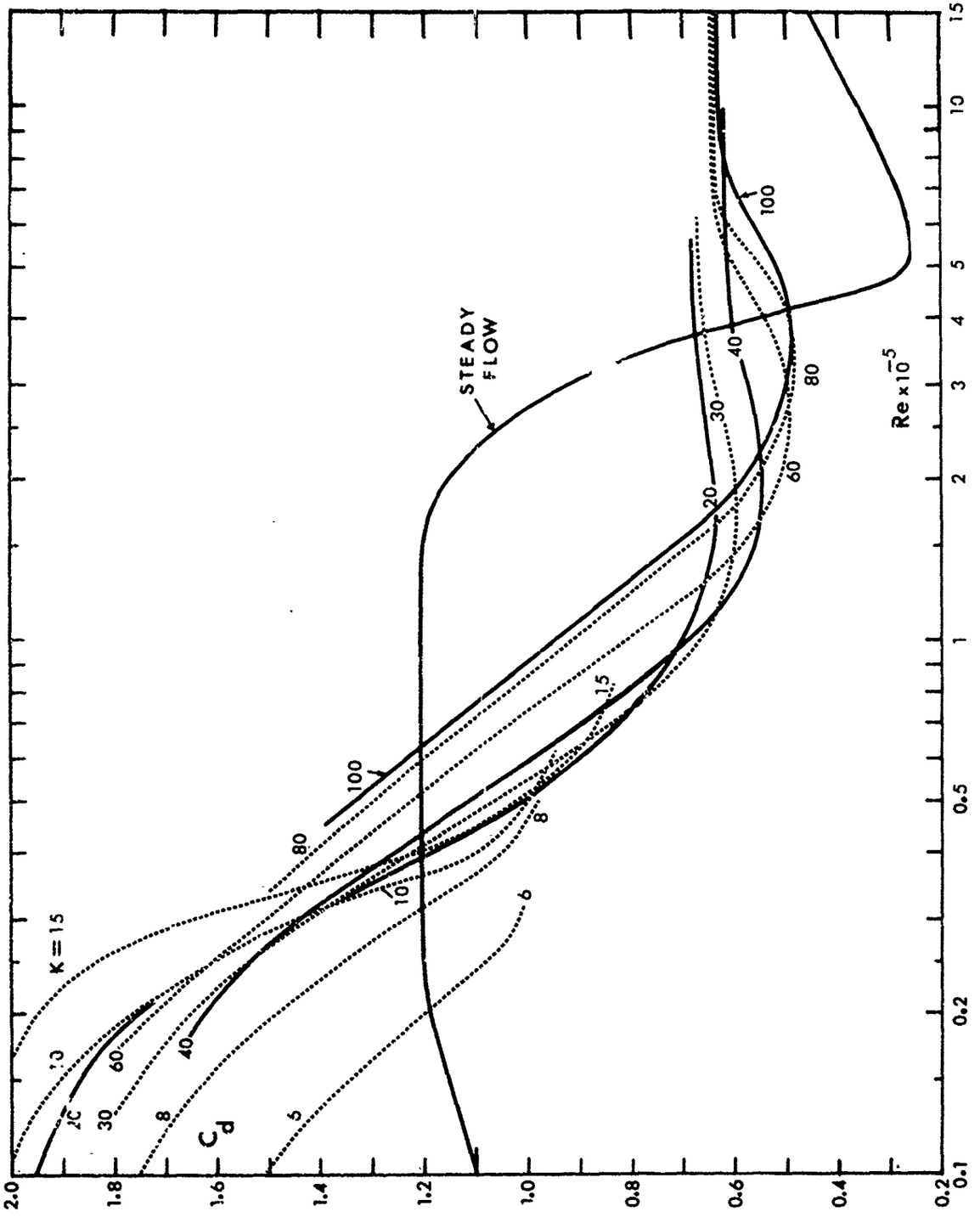

Fig. 12 C_d versus Re for constant values of K, (Present data).

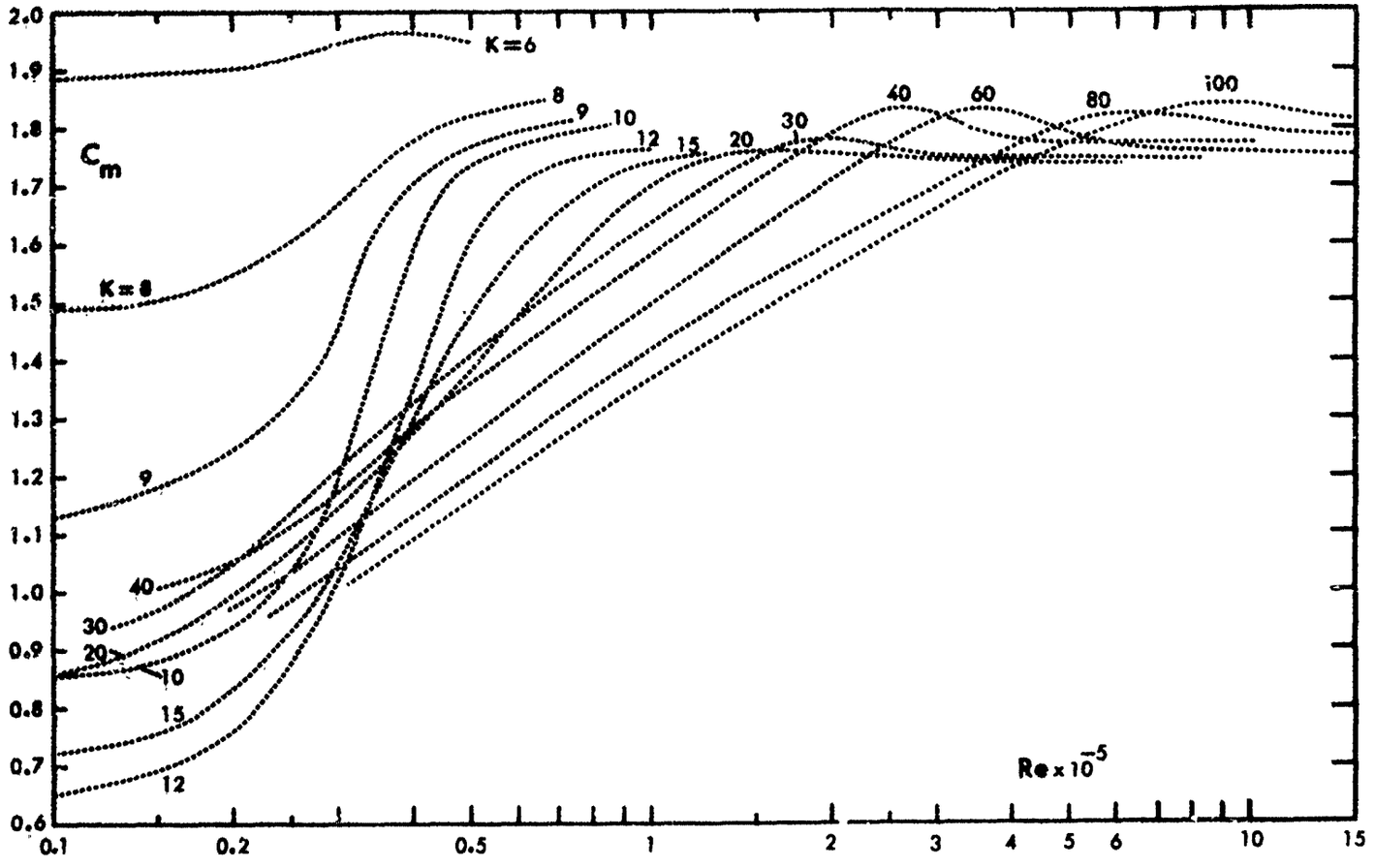

Fig. 13 C_m versus Re for constant values of K, (Present data).

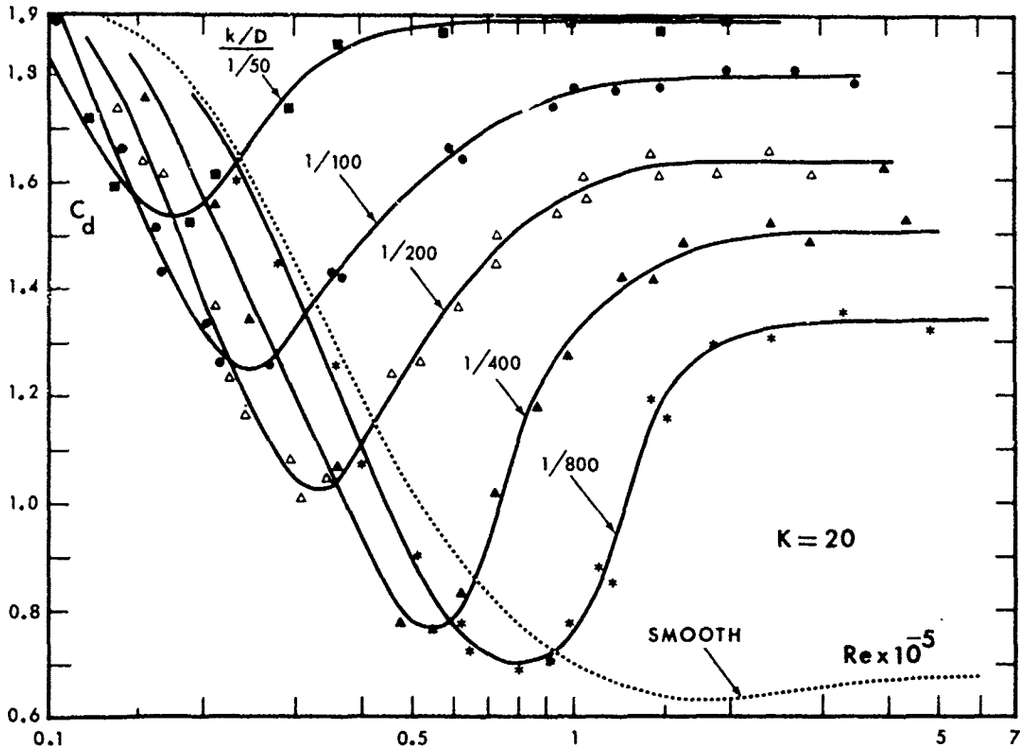

Fig. 14a C_d versus Re for various values of k/D, (K = 20).

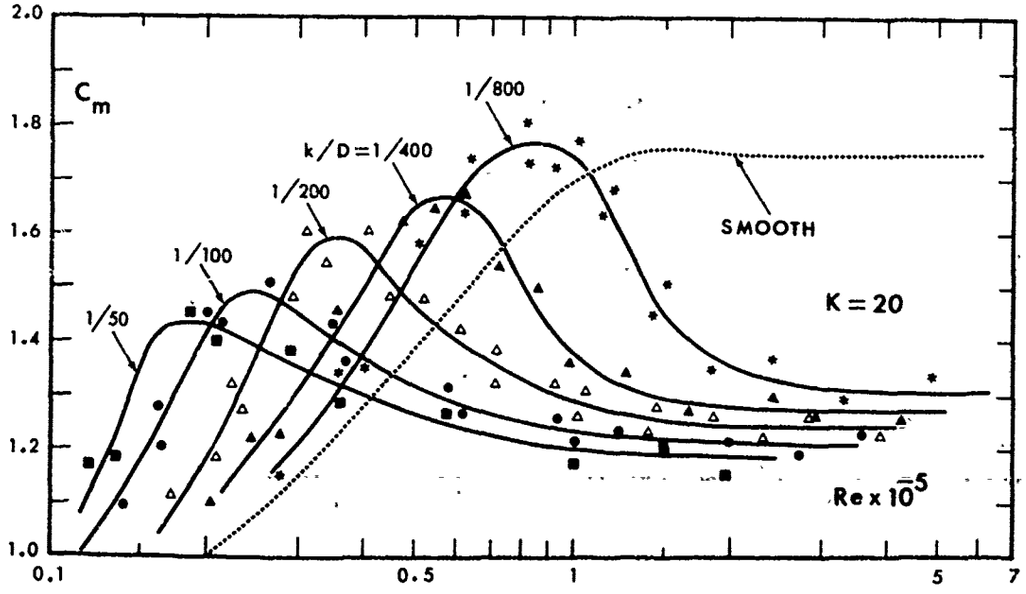

Fig. 14b C_m versus Re for various values of k/D, (K = 20).

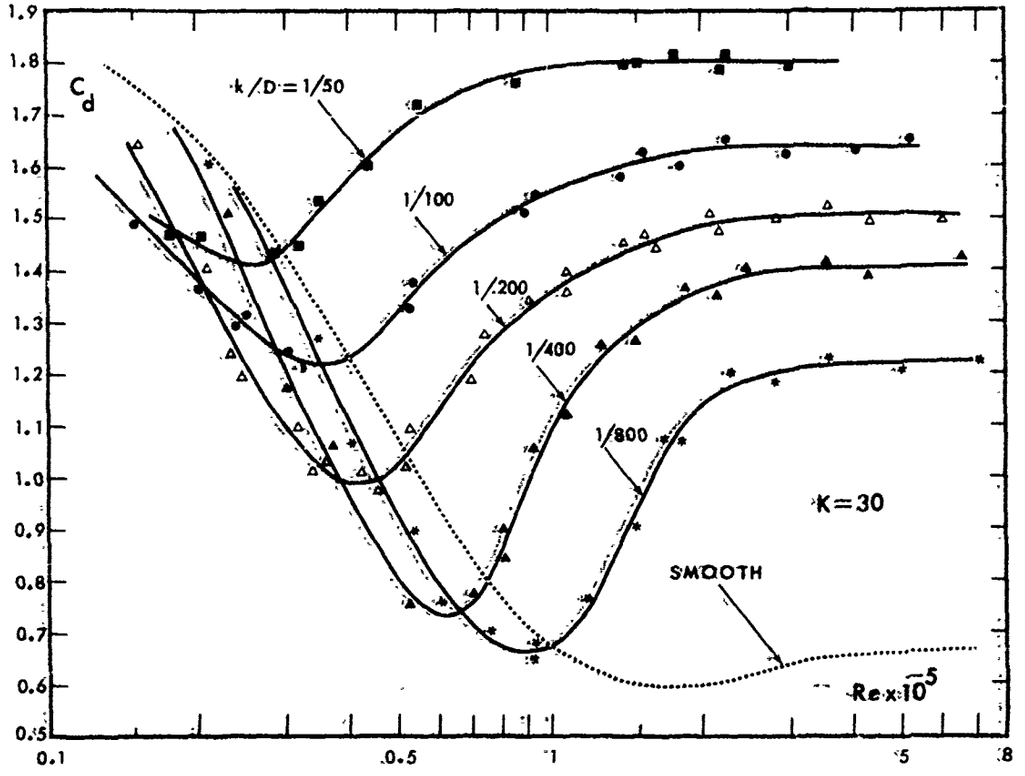

Fig. 15a C_d versus Re for various values of k/D, (K = 30).

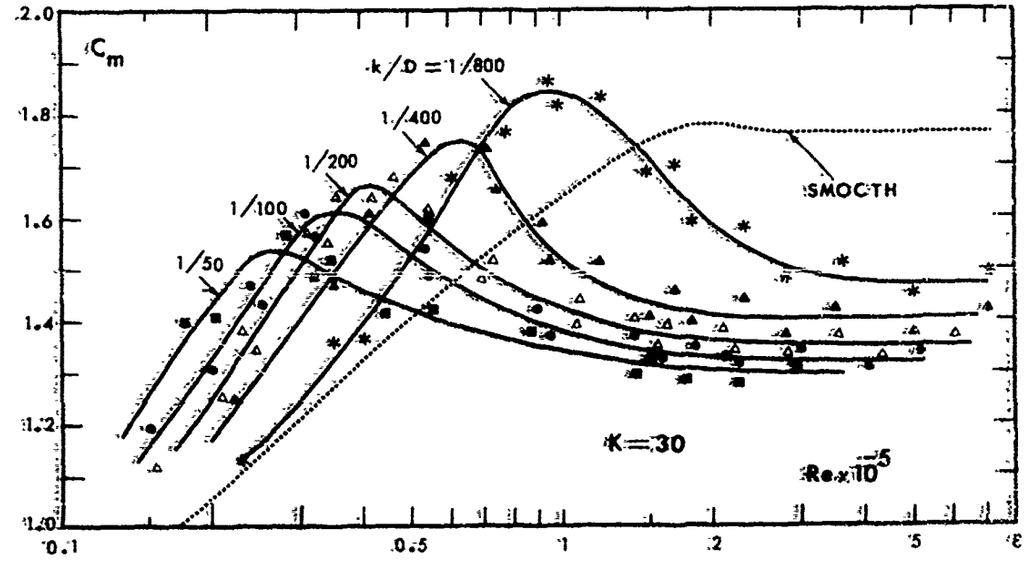

Fig. 15b C_m versus Re for various values of k/D, (K = 30).

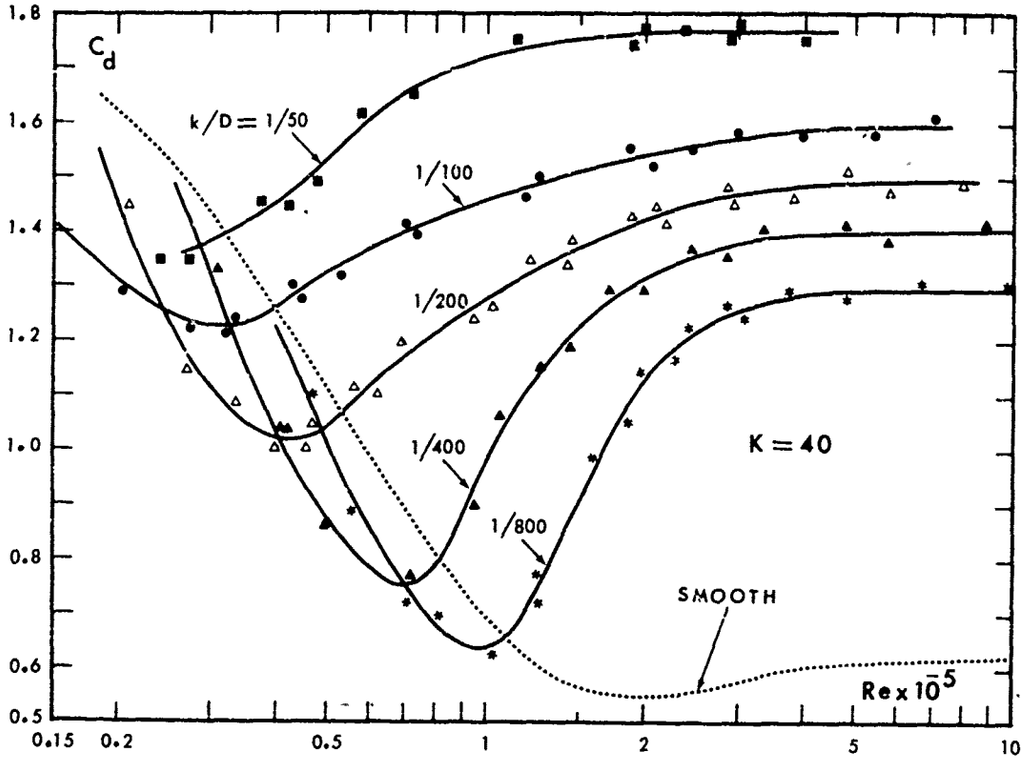

Fig. 16a C_d versus Re for various values of k/D, (K = 40).

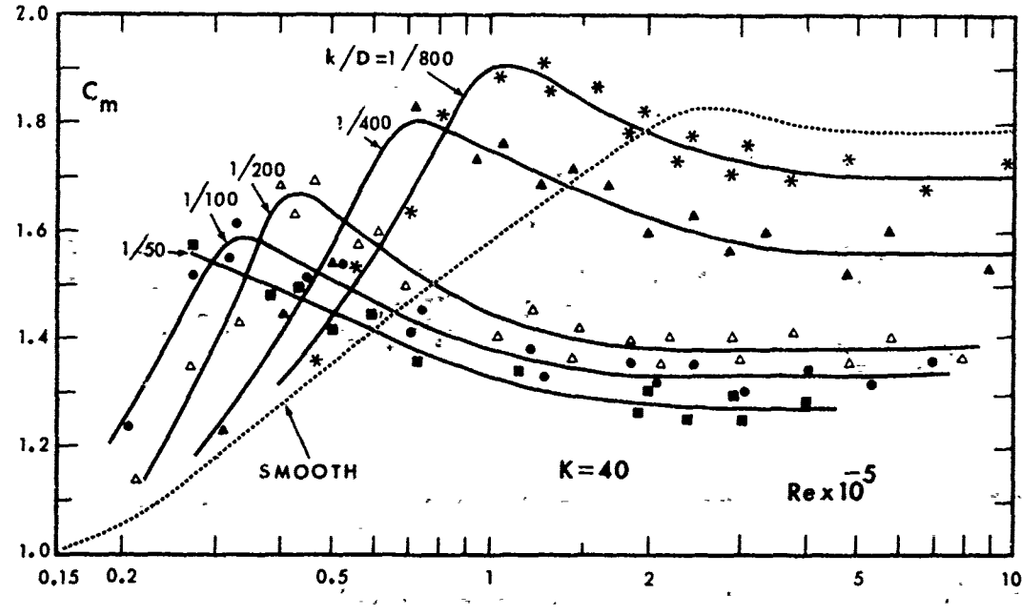

Fig. 16b C_m versus Re for various values of k/D, (K = 40).

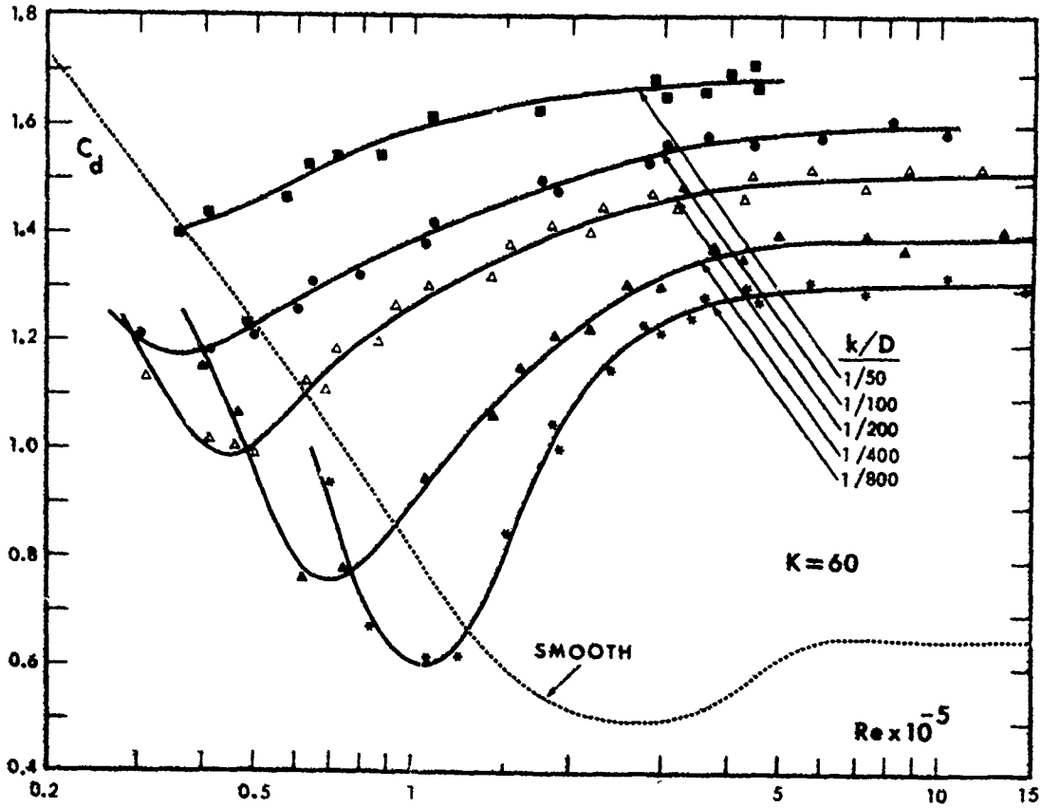

Fig. 17a C_d versus Re for various values of k/D, (K = 60).

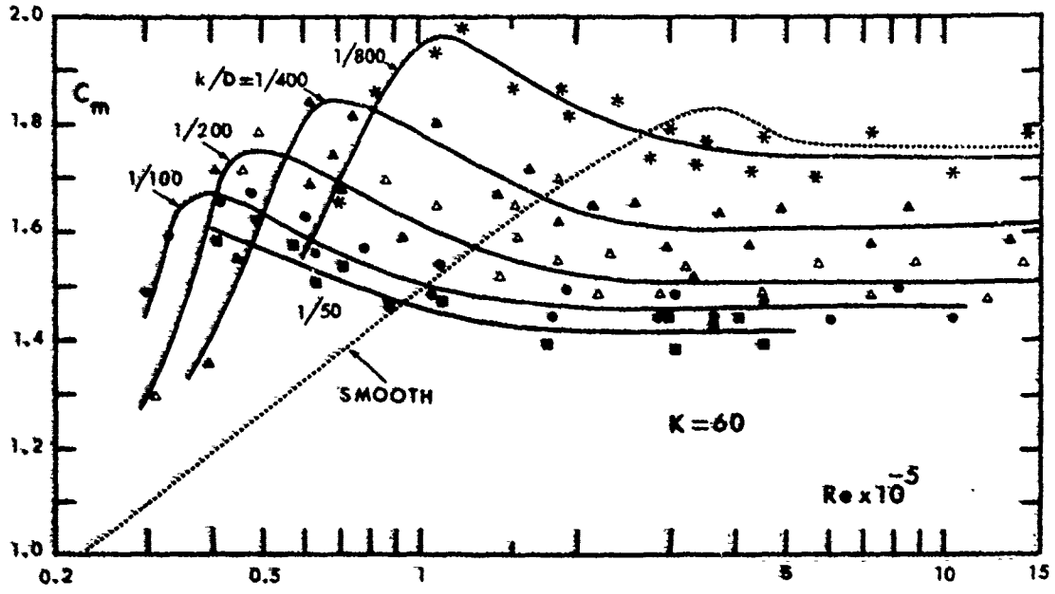

Fig. 17b C_m versus Re for various values of k/D, (K = 60).

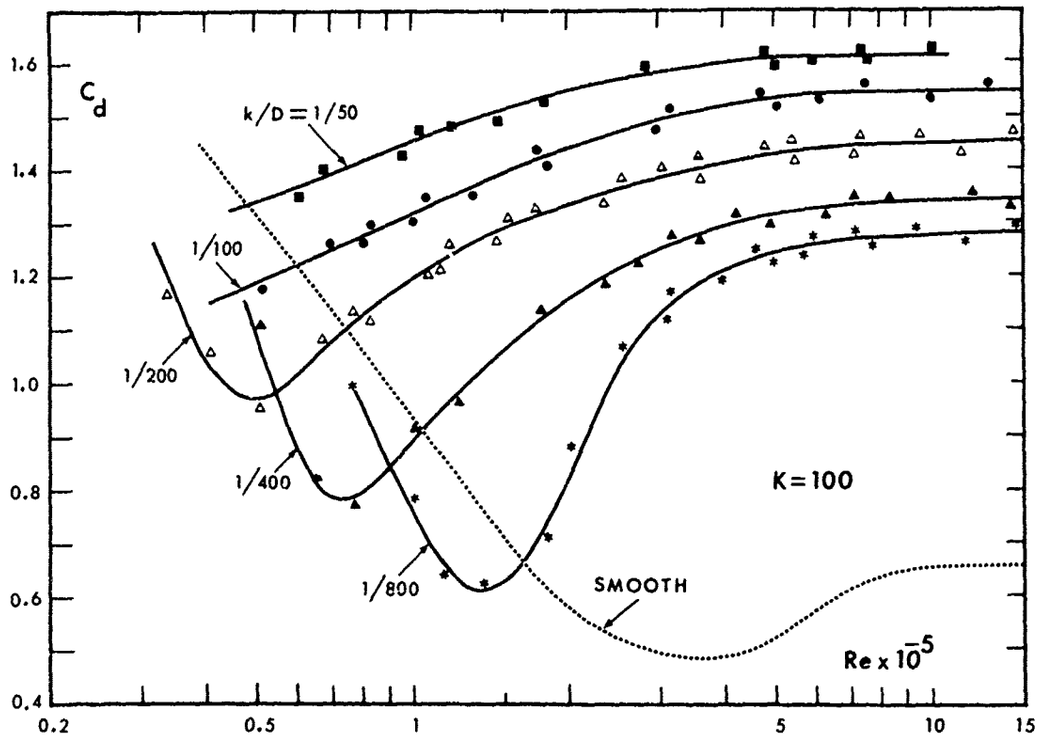

Fig. 18a C_d versus Re for various values of k/D, (K = 100).

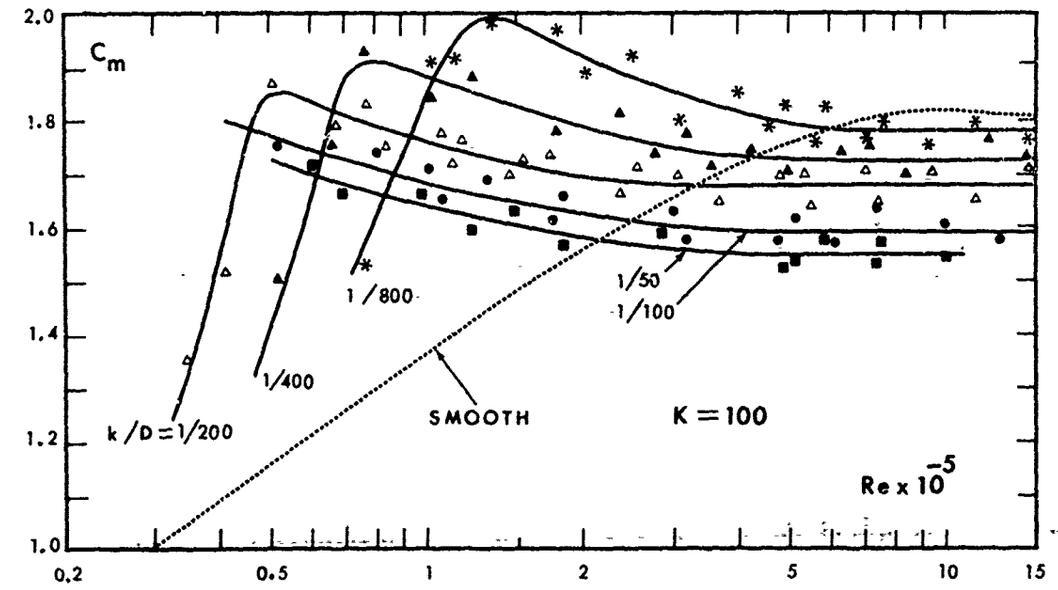

Fig. 18b C_m versus Re for various values of k/D, (K = 100).

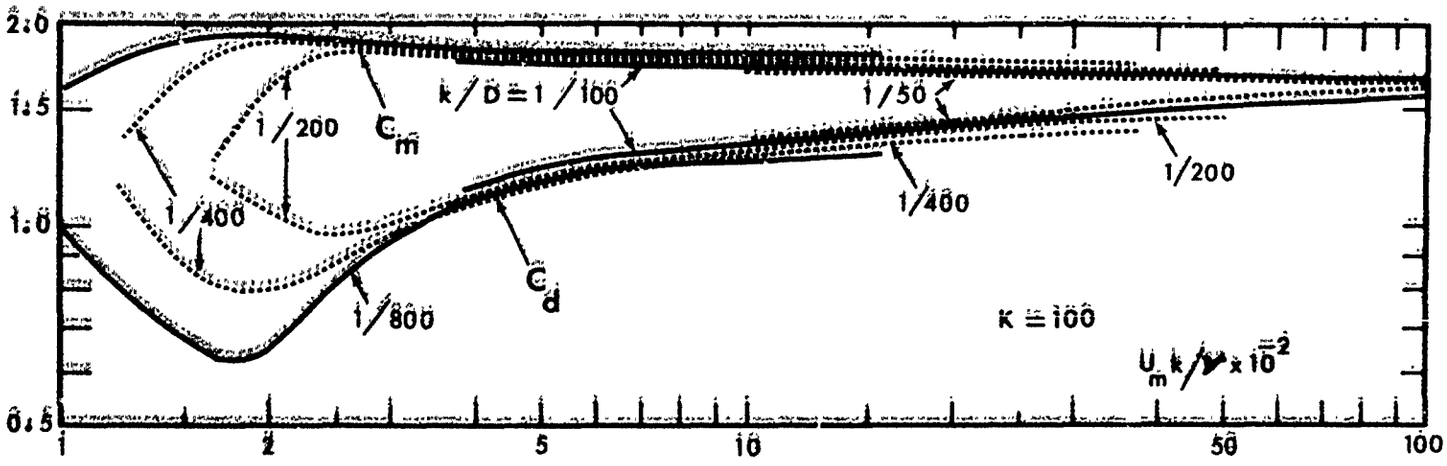

Fig. 19 Drag and inertia coefficien[illegible]tion of the roughness Reynolds number for various values o[illegible] for K = 100.

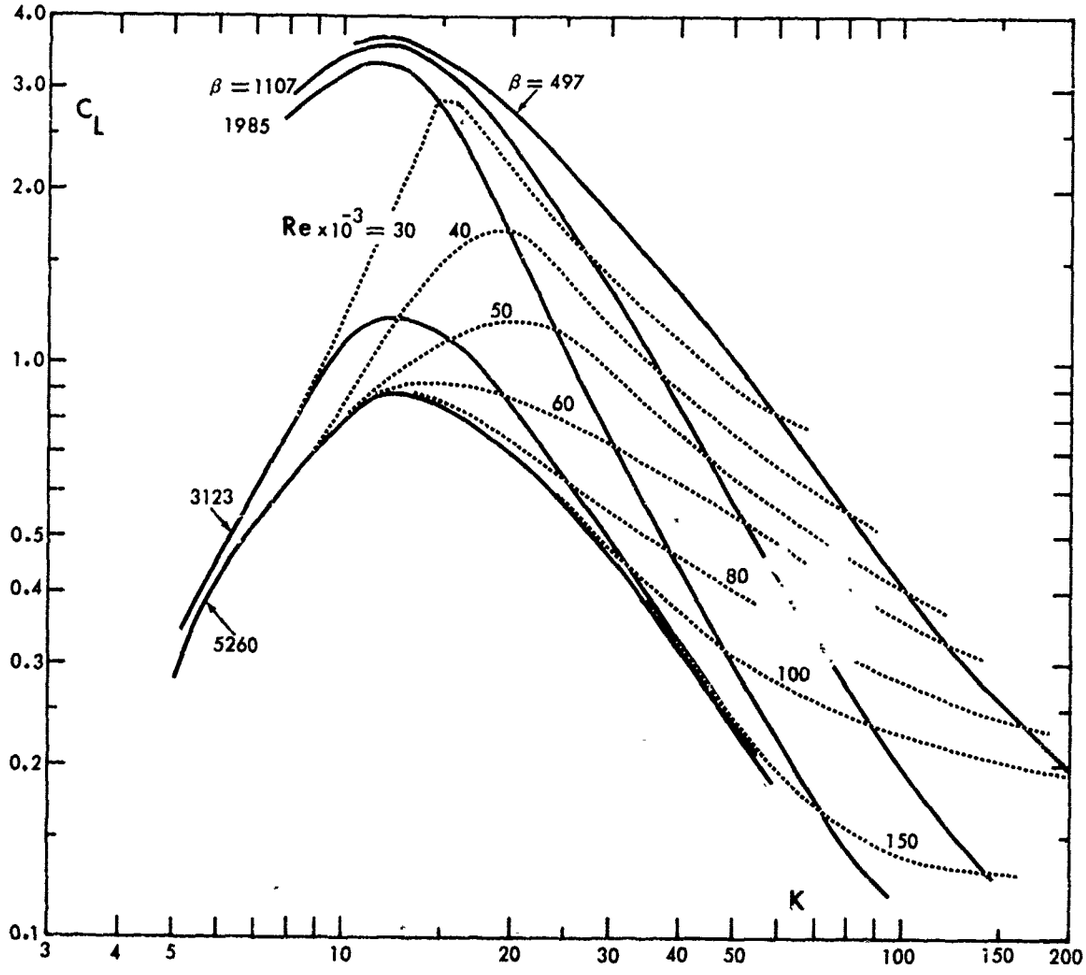

Fig. 20 C_L versus K for various values of Re and β (smooth cylinders)

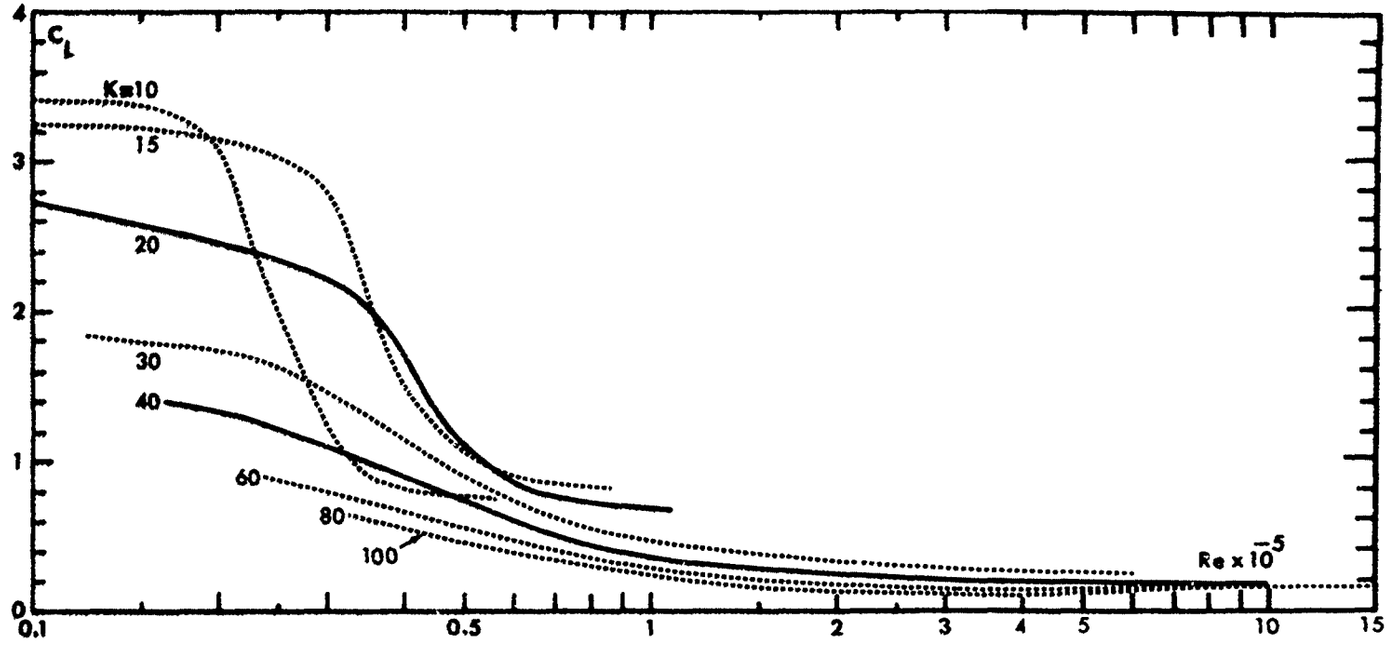

Fig. 21 Maximum lift coefficient versus Reynolds number for various values of K

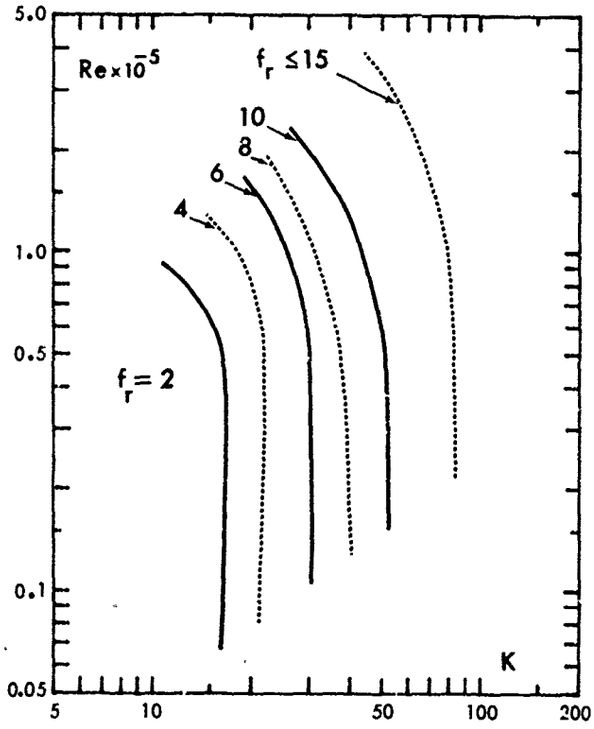

Fig. 22 f_r as a function of Re and K
(smooth cylinder data)

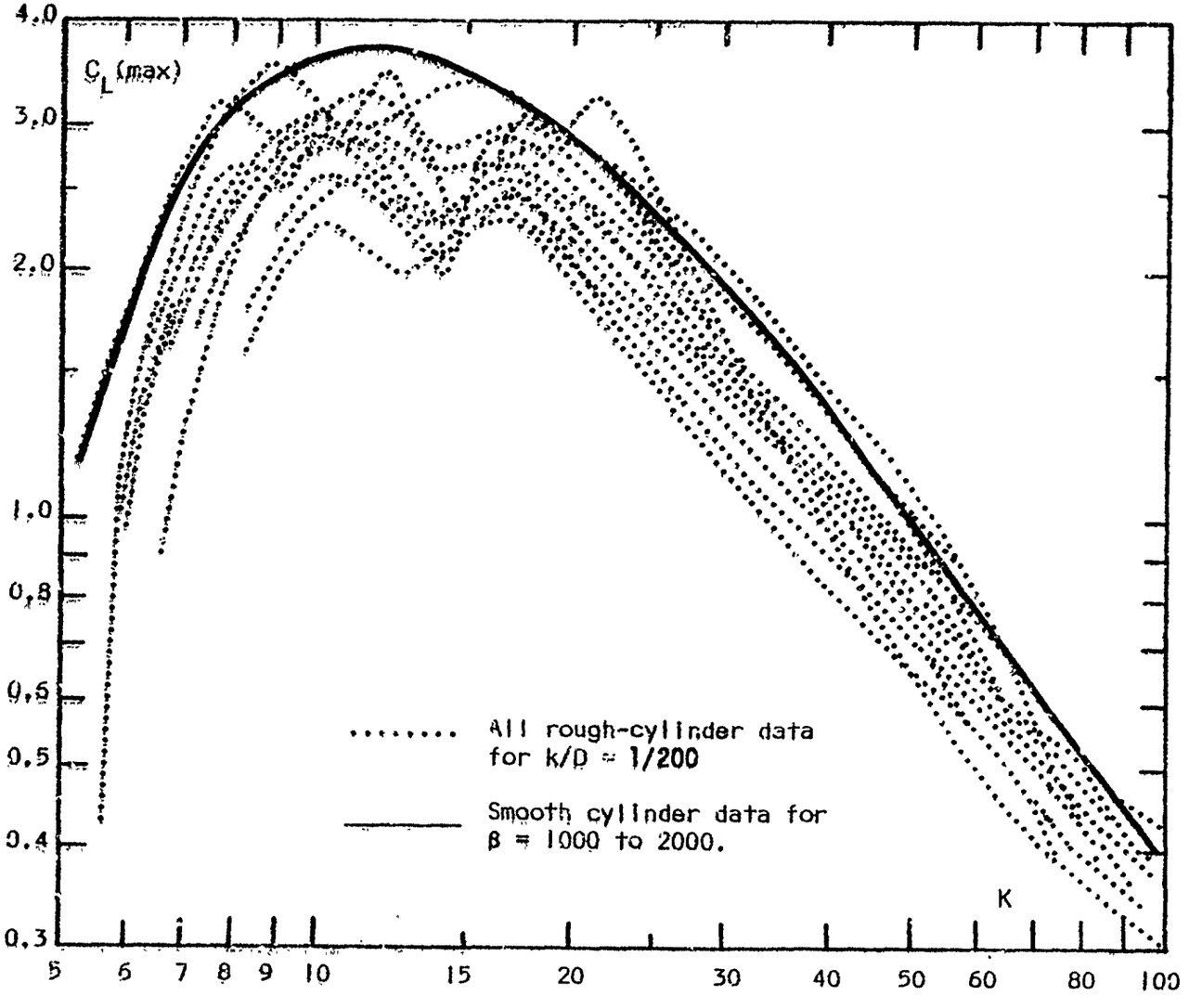

Fig. 23a Combined plot of C_L(max) data for k/D = 1/200 for various values of β

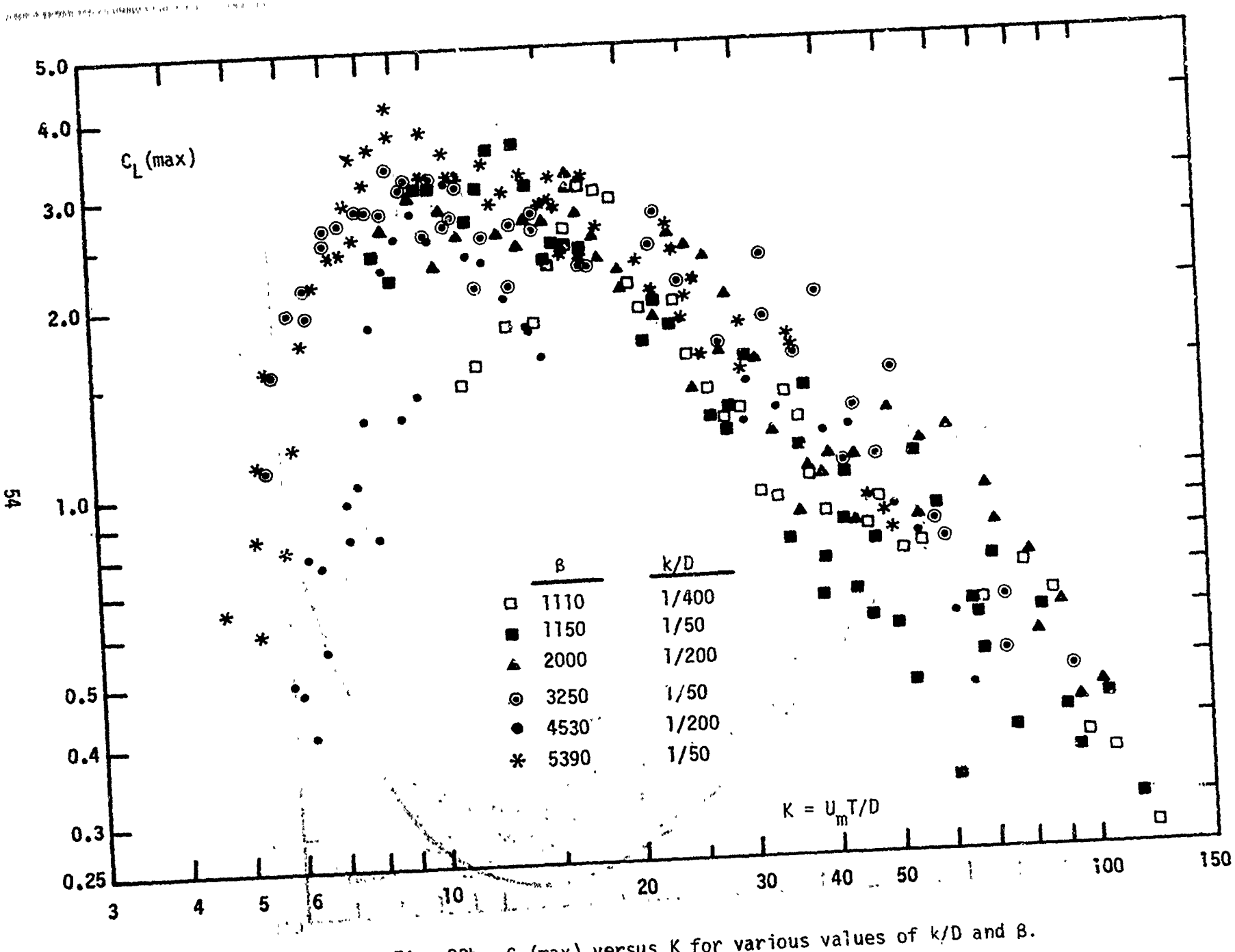

Fig. 23b C_L(max) versus K for various values of k/D and β.

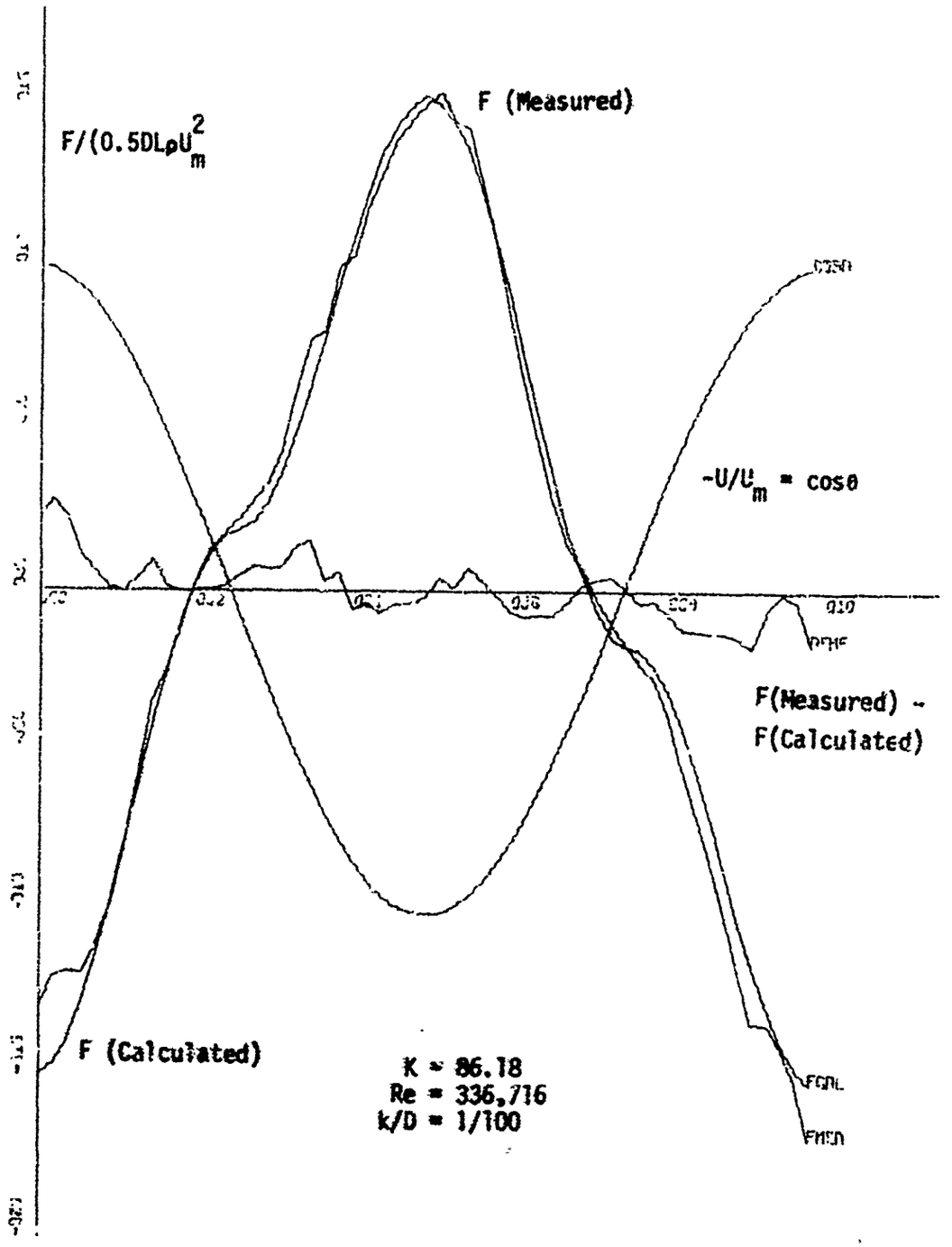

Fig. 24a Comparison of measured and calculated forces.

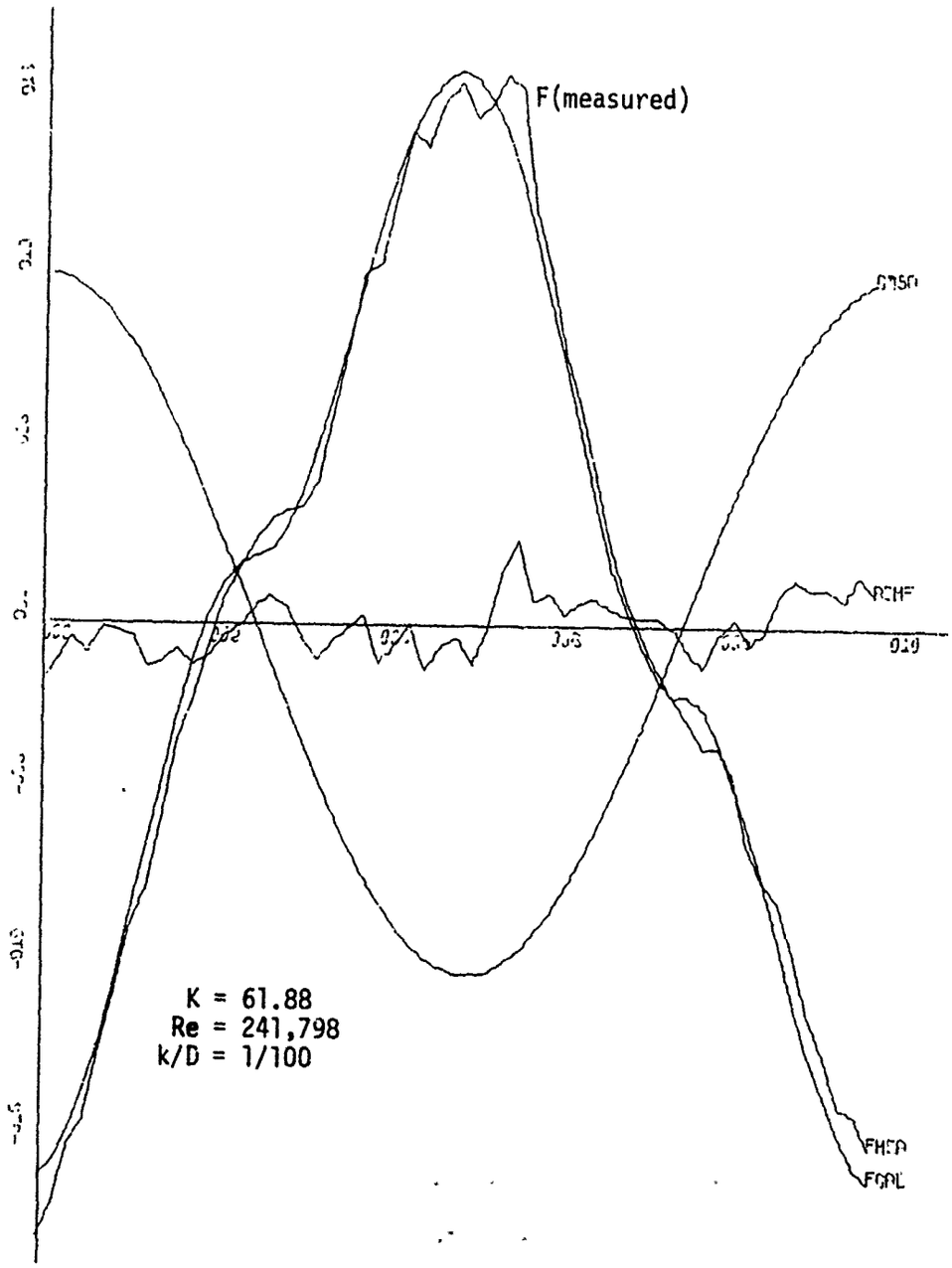

Fig. 24b Comparison of measured and calculated forces

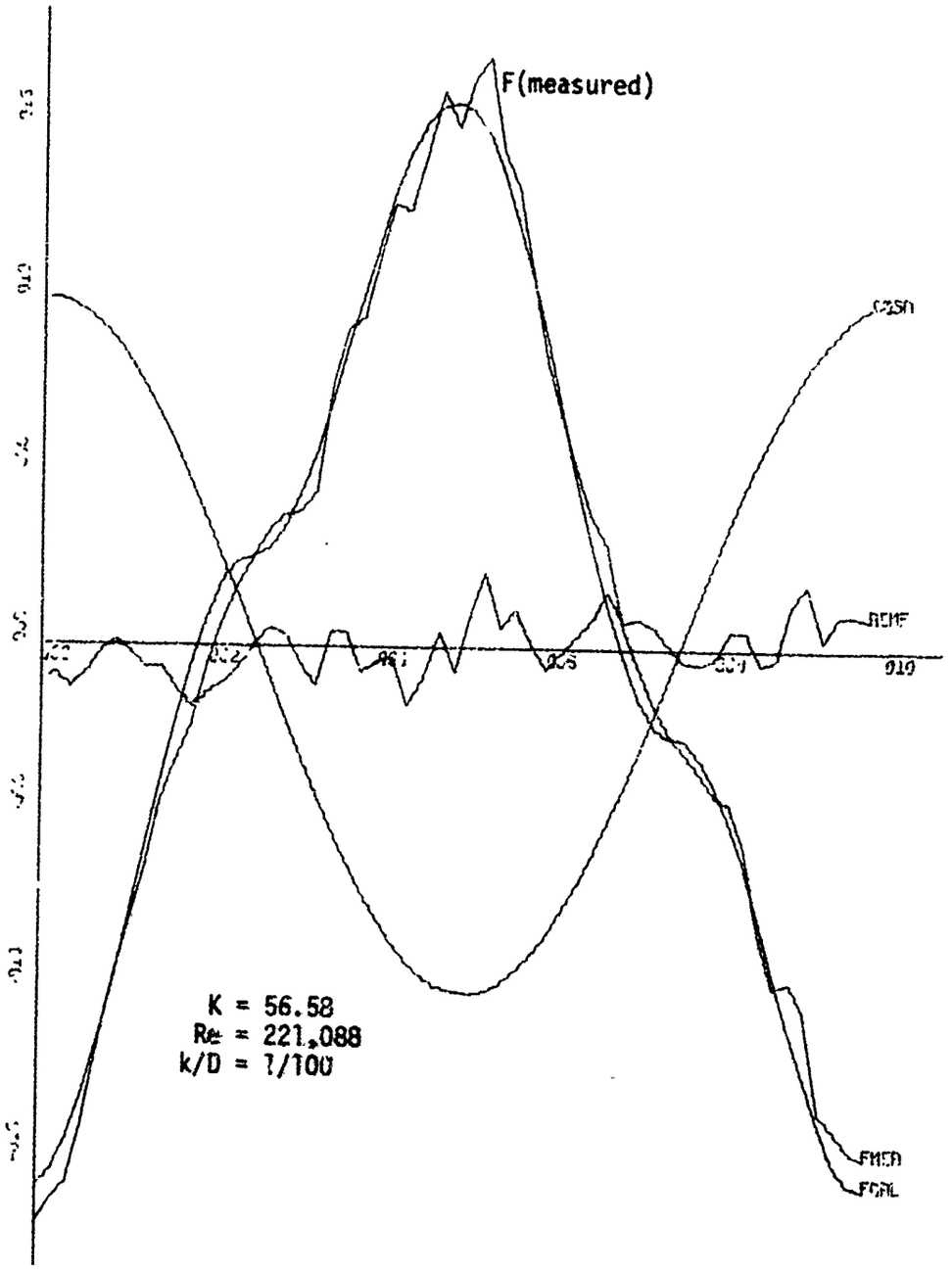

Fig. 24c Comparison of measured and calculated forces.

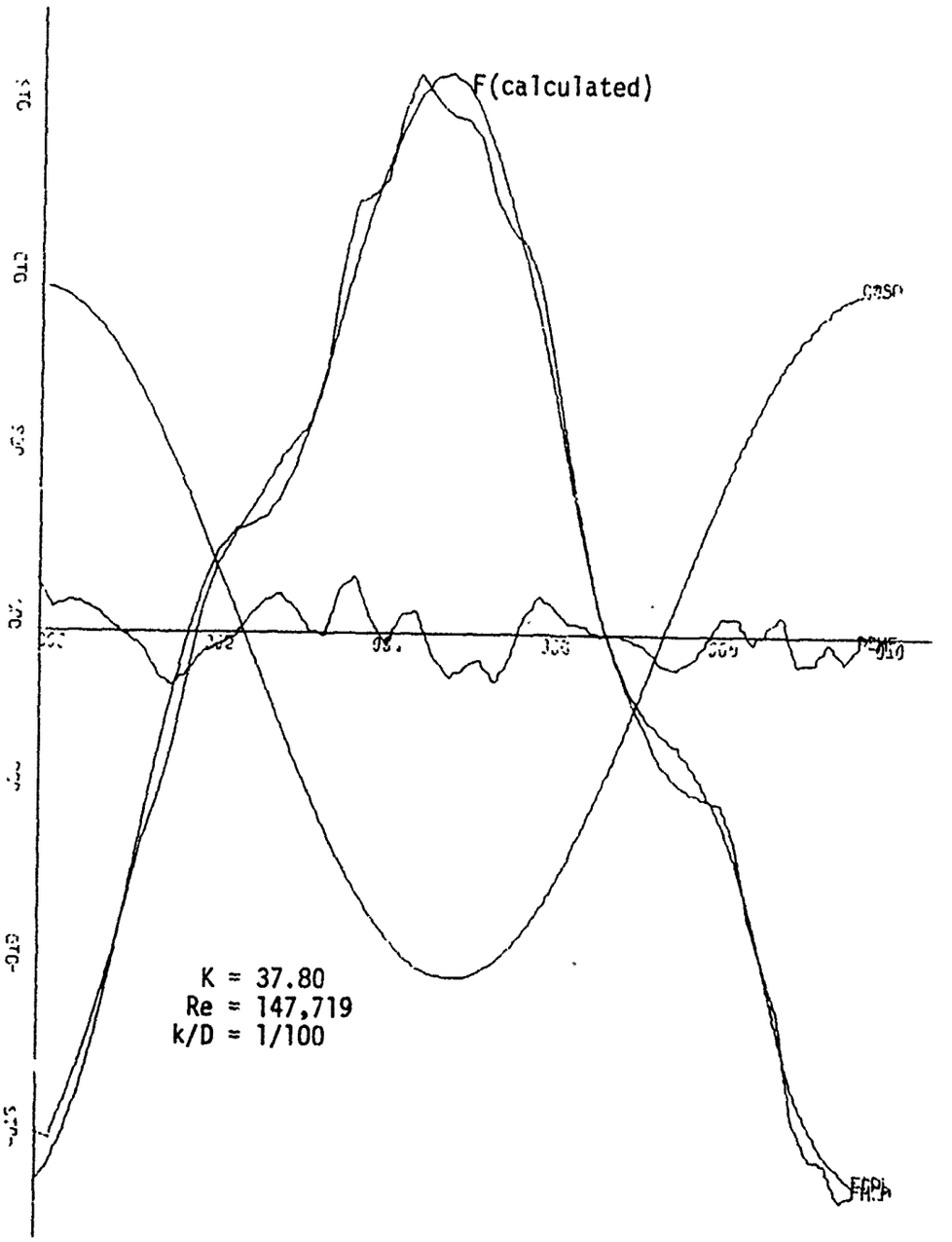

Fig. 24d Comparison of measured and calculated forces

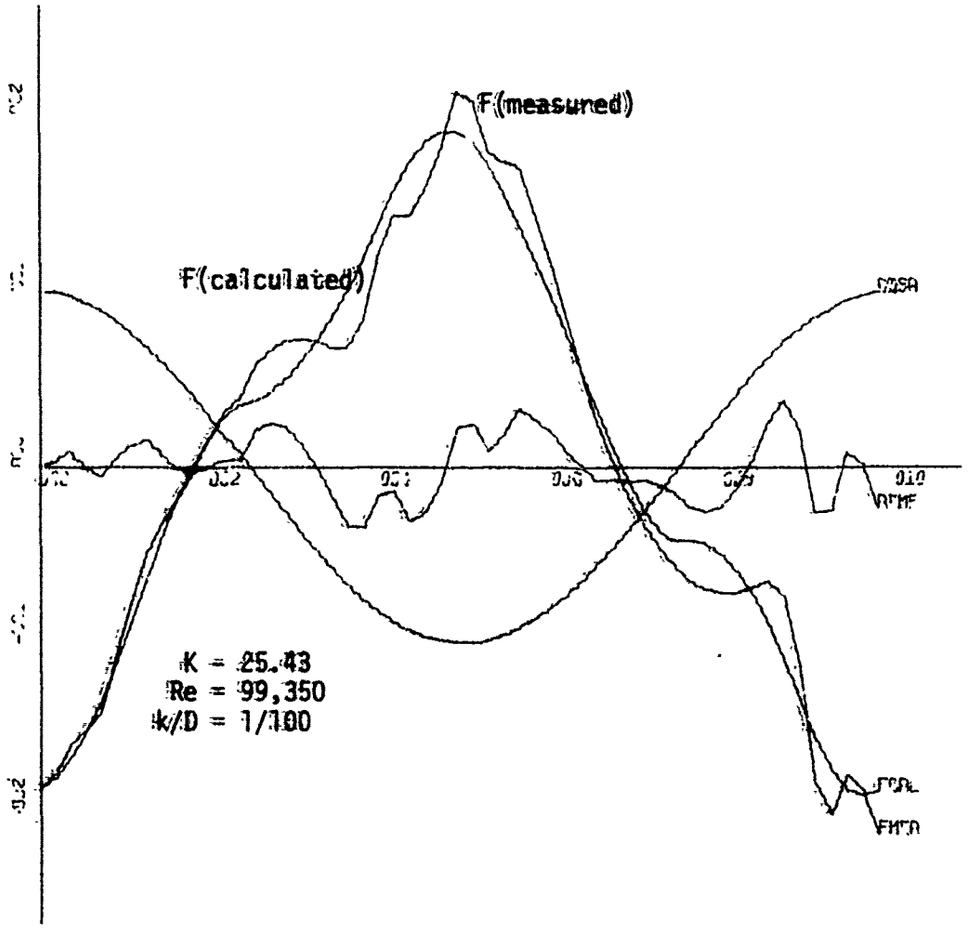

Fig. 24e Comparison of measured and calculated forces

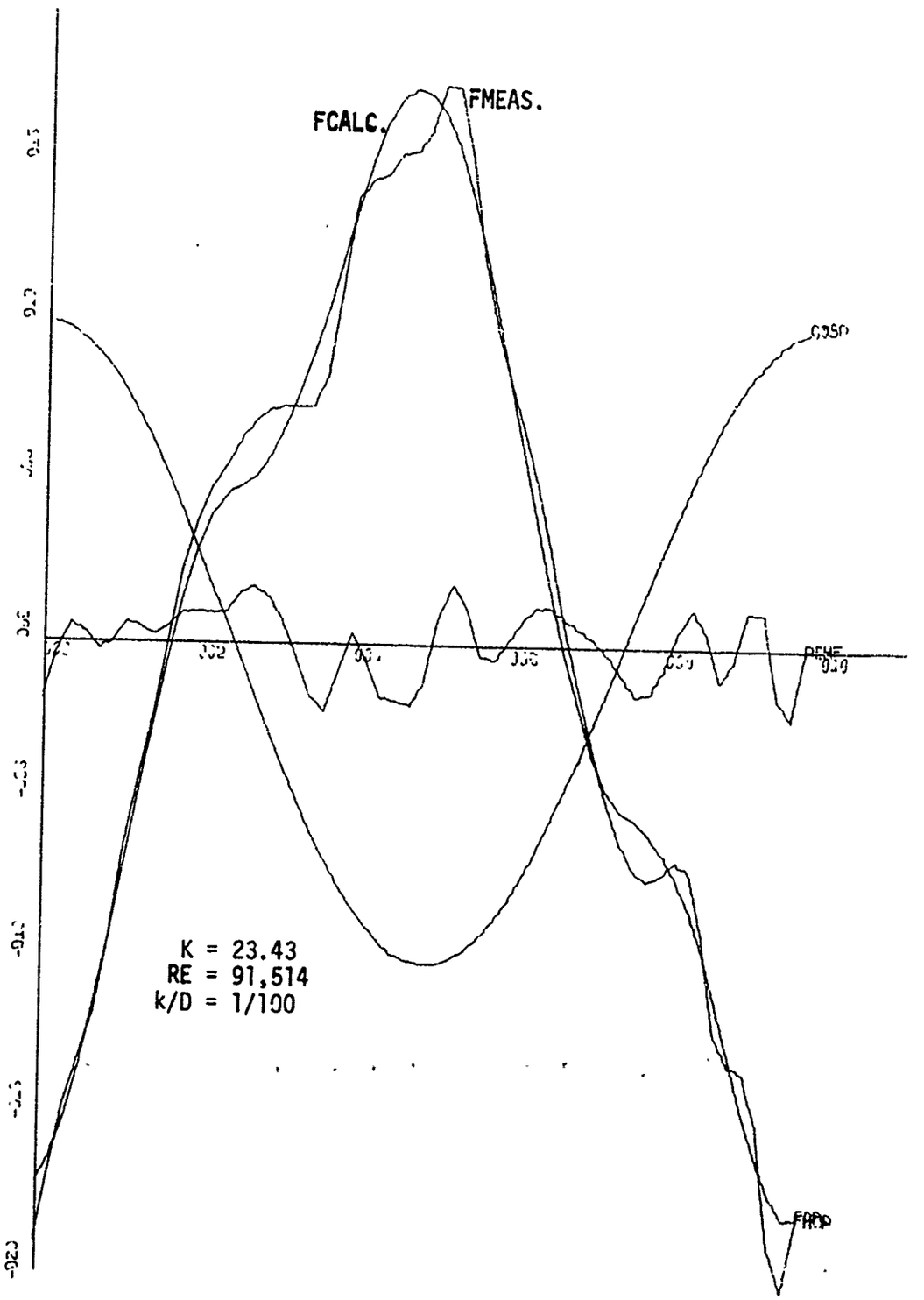

Fig. 24f Comparison of measured and calculated forces

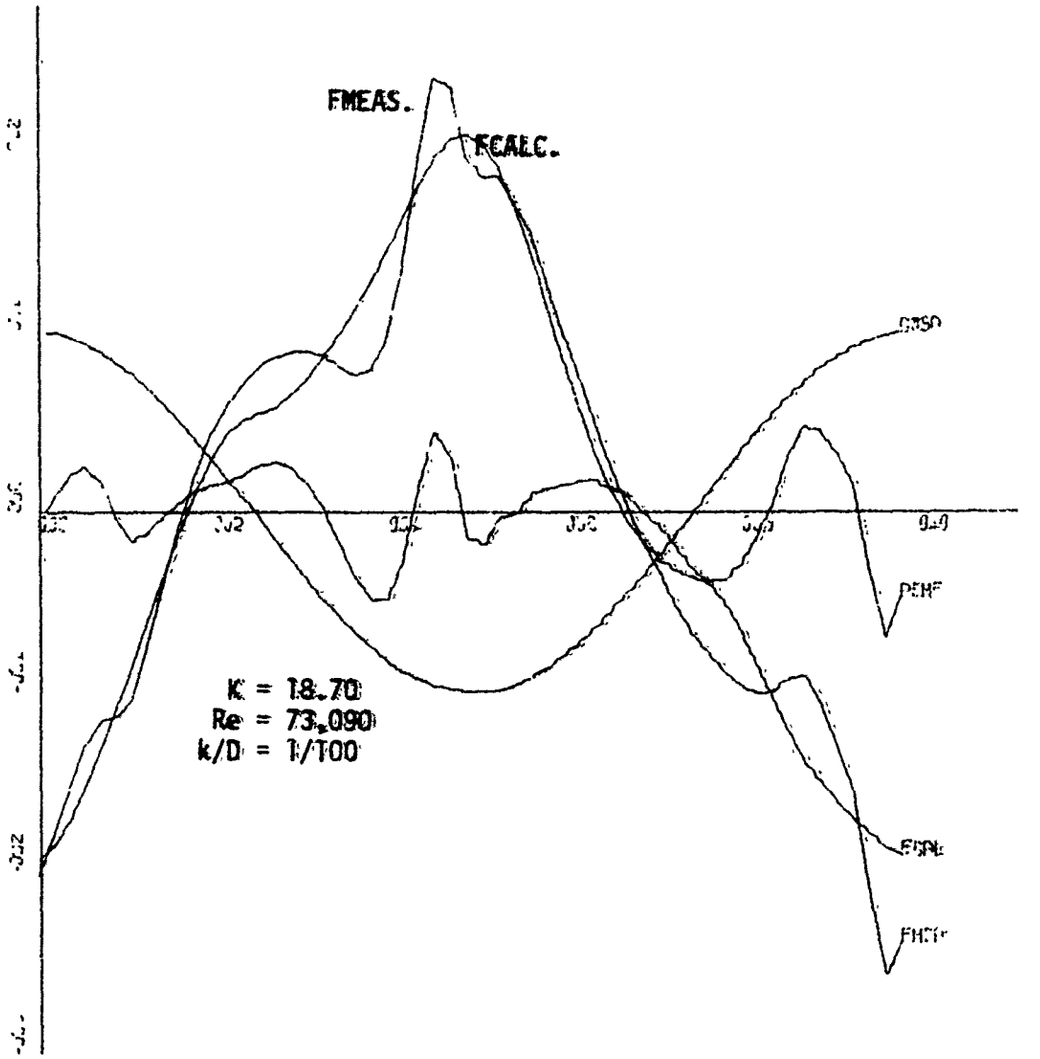

Fig. 24g Comparison of measured and calculated forces

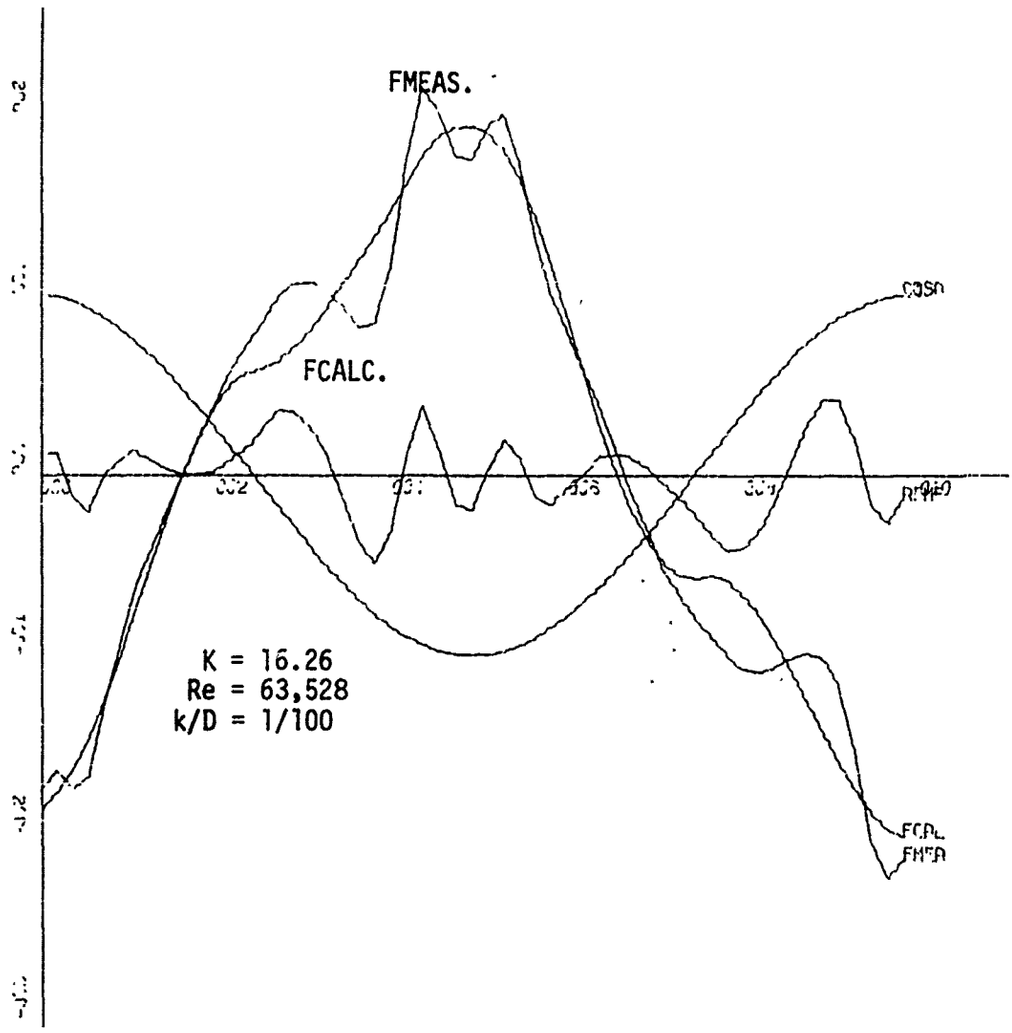

Fig. 24h Comparison of measured and calculated forces

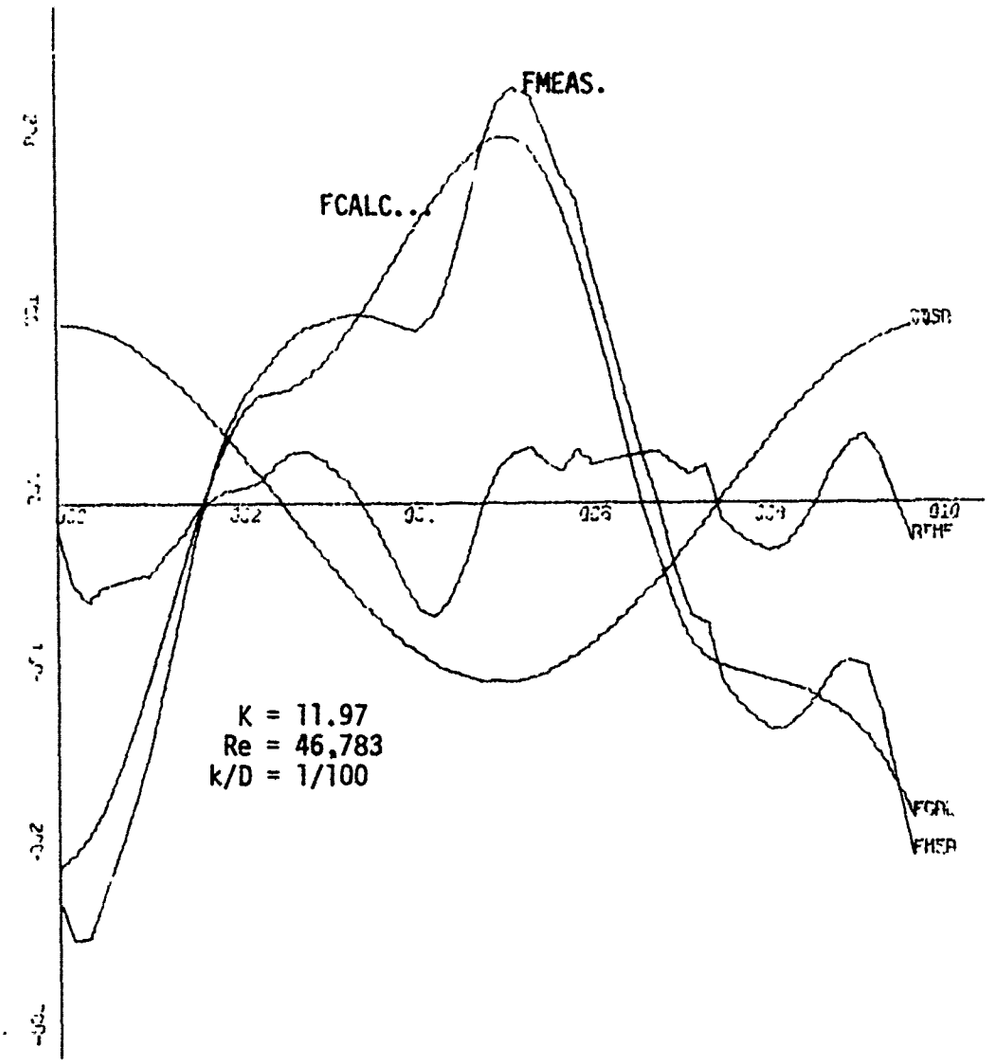

Fig. 24i Comparison of measured and calculated forces

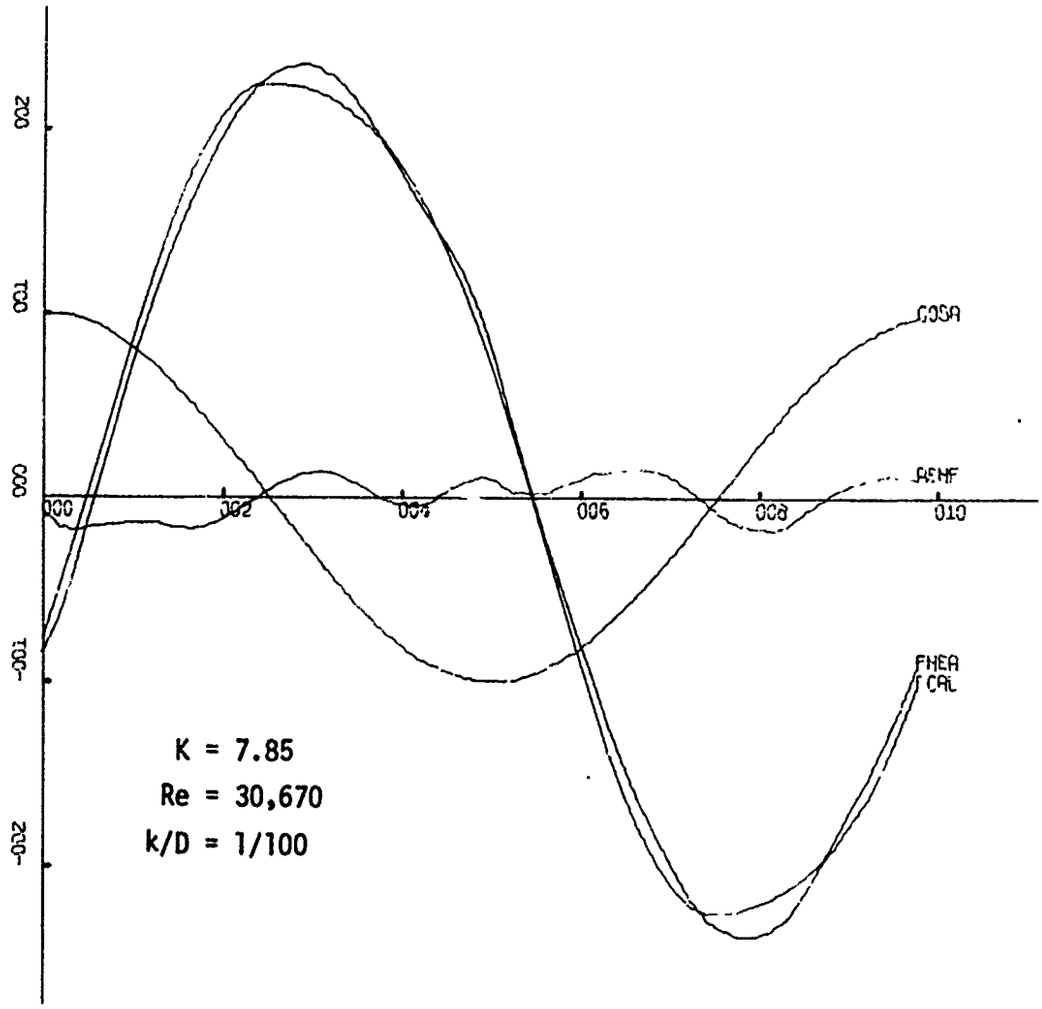

Fig. 24j Comparison of measured and calculated forces

INITIAL DISTRIBUTION LIST

		No. Copies
1.	Defense Documentation Center Cameron Station Alexandria, Virginia 22314	12
2.	National Science Foundation Washington, D. C. 20550 ATTN: Dr. George K. Lea	2
3.	Dean of Research Naval Postgraduate School Monterey, Calif. 93940	1
4.	Chairman, Department of Mechanical Engineering, Code: 59 Naval Postgraduate School Monterey, Calif. 93940	2
5.	Library, Code 0212 Naval Postgraduate School Monterey, Calif. 93940	2
6.	Prof. T. Sarpkaya, Code: 59SL Mechanical Engineering Naval Postgraduate School Monterey, Calif. 93940	20
7.	National Physical Laboratory Division of Maritime Science Teddington, Middlesex England ATTN: Superintendent N. Hogben B. L. P. Miller	3
8.	Prof. Robert A. Grace Department of Ocean Engineering University of Hawaii Honolulu, Hawaii	1
9.	Prof. R. L. Wiegel Hydraulic Engineering Lab. University of California Berkeley, California	1
10.	Prof. Charles Dalton Mechanical Engineering University of Houston Houston, Texas	1

		No. Copies
11.	Dr. Yoshimi Goda Marine Hydrodynamics Division Port and Harbour Institute Ministry of Transport Nagase, Yokosuka, Japan	1
12.	Prof. Yuichi Iwagaki Civil Engineering Kyoto University Kyoto, Japan	1
13.	Prof. John H. Nath Mechanical Engineering/Oceanography Oregon State University Corvallis, Oregon	1
14.	Prof. Yoshito Tsuchiya Disaster Prevention Research Institute Kyoto University Kyoto, Japan	1
15.	Prof. Robert G. Dean Ocean Engineering University of Delaware Newark, Delaware	1
16.	Prof. John S. McNown College of Engineering University of Kansas Lawrence, Kansas	1
17.	Dr. D. J. Maull Engineering Department University of Cambridge Trumpington Street Cambridge, England	1
18.	British Hydromechanics Research Association Cranfield, Bedford England	1
19.	Dr. John A. Mercier CONACO P. O. Box 2197 Houston, Texas 77001	1
20.	Dr. M. M. Zdravkovich Mechanical Engineering University of Salford Salford M5 4WT, England	1

		No. Copies
21.	National Science Foundation Engineering Division Library 1800 G Street, N.W. Washington, D.C. 20550	20
22.	Commanding Officer (L31) Naval Civil Engineering Lab. Port Hueneme, California 93043	1
23.	Commander Naval Undersea Research and Development Center San Diego, California 92132 ATTN: Dr. A. Fabula	1
24.	Officer-in-Charge Naval Undersea Research and Development Center Pasadena, California 91107 ATTN: Library (13111)	1
25.	Research Center Library Waterways Experiment Station Corp. of Engineers P.O. Box 631 Vicksburg, Mississippi 39180	1
26.	National Bureau of Standards Washington, D.C. ATTN: G. Kulin Fluid Mechanics Hydraulic Section	1
27.	Assistant Chief Design Eng. for Naval Architecture Code 250 Mare Island Naval Shipyard Vallejo, California 94592	1
28.	U. S. Merchant Marine Academy Kings Point, L.I., New York 11204 ATTN: Academy Library	1
29.	Hydronautics, Inc. Pindell School Road Howard County Laurel, Maryland 20810 ATTN: Library	1
30.	Oceanics, Inc. Technical Industrial Park Plainview, L.I., New York 11803	1

		No. Copies
31.	Commander Naval Ship Research and Development Center Bethesda, Maryland 20034 ATTN: Code 1505	1
32.	Officer-in-Charge Annapolis Laboratory Naval Ship Research and Development Center Annapolis, Maryland 21402 ATTN: Code 5642 (Library)	1
33.	Commander Naval Sea Systems Command Washington, D.C. 20362 ATTN: SEA 033	1
34.	Director Defense Documentation Center 5010 Duke Street Alexandria, Virginia 22314	1
35.	Office of Naval Research 800 North Quincy Street Arlington, Virginia 22217 ATTN: Mr. R. D. Cooper Code 438	1
36.	Chief Scientist Office of Naval Research Branch Office 1030 E. Green Street Pasadena, California 91106	1
37.	Office of Naval Research San Francisco Area Office Room 447 760 Market Street San Francisco, California 94102	1
38.	Director Naval Research Laboratory Washington, D.C. 20390 ATTN: Code 2027	1
39.	Commander Naval Facilities Engineering Command (Code 032C) Washington, D.C. 20390	1
40.	Library of Congress Science & Technology Division Washington, D.C. 20540	1

		No. Copies
41.	Society of Naval Architects and Marine Engineers 74 Trinity Place New York, New York 10006 ATTN: Technical Library	1
42.	Stevens Institute of Technology Davidson Laboratory 711 Hudson Street Hoboken, New Jersey 07030 ATTN: Prof. J. Breslin, Director	1
43.	Stanford University Department of Civil Engineering Stanford, California 94305 ATTN: Prof. R. L. Street	1
44.	Southwest Research Institute P.O. Drawer 28510 San Antonio, Texas 78284 ATTN: Applied Mech. Review Dr. H. Abramson	1
45.	Ocean Engineering Department Woods Hole Oceanographic Institute Woods Hole, Massachusetts 02543	1
46.	University of California College of Engineering Berkeley, California 94720 ATTN: Library Prof. J. Wehausen	1
47.	Harvard University Pierce Hall Cambridge, Massachusetts 02138 ATTN: Gordon McKay Library	1
48.	University of Hawaii Department of Ocean Engineering 2565 The Mall Honolulu, Hawaii 96822 ATTN: Dr. C. Bretschneider	1
49.	University of Illinois Urbana, Illinois 61801 ATTN: Dr. J. Robertson	1
50.	Department of Ocean Engineering Massachusetts Institute of Technology Cambridge, Massachusetts 02139 ATTN: Department Library	1

No. Copies

51. Webb Institute of Naval Architecture
Crescent Beach Road
Glenn Cover, L.I., New York 11542
ATTN: Library 1

52. St. Anthony Falls Hydraulic Lab
University of Minnesota
Mississippi River at 3rd Avenue, S.E.
Minneapolis, Minnesota 55414
ATTN: Library 1

53. Department of Naval Architecture and Marine Engineering
Ann Arbor, Michigan 48104
ATTN: Library 1

54. Davidson Laboratory
Stevens Institute of Technology
711 Hudson Street
Hoboken, New Jersey 07030
ATTN: Library 1

55. Department of Ocean Engineering
Massachusetts Institute of Technology
Cambridge, Massachusetts 02139
ATTN: Prof. J. N. Newman 1

56. Hydronautics, Inc.
Laurel, Maryland 20810
ATTN: Dr. M. P. Tulin 1

57. Library (Code 1640)
Naval Oceanographic Office
Washin on, D.C. 20390 1

58. Department of Ocean Engineering
Massachusetts Institute of Technology
Cambridge, Mass. 02139
ATTN: Prof. Jerome H. Milgram 1

59. Prof. Michael S. Longuet-Higgins
University of Cambridge
1 Long Road
Cambridge CB2 2PP, England 1

60. Professor T. Carstens
The River and Harbour Laboratory
The Norwegian Institute of Technology
7034 Trondheim - NTH
Norway 1